November 18, 2003
WOG-03-608

WCAP-15872-NP
Project Number 694

U. S. Nuclear Regulatory Commission
Attention: Document Control Desk
Washington, DC 20555-0001

Attention: Chief, Information Management Branch
Division of Program Management

Subject: **Response to Request for Additional Information – WCAP-15872-NP, Rev. 0, "Use of Alternate Decay Heat Removal in Mode 6 Refueling,"**

References:

1. NRC Letter, D. Holland (NRC) to G. Bischoff (Westinghouse), "Request for Additional Information – WCAP-15872-NP, Revision 0, Use of Alternate Decay Heat Removal In Mode 6 Refueling," (TAC No. MB9020), October 2, 2003.

2. WOG Letter, R. H. Bryan to US NRC Document Control Desk, "Transmittal of Report WCAP-15872, Rev 00 (Non-Proprietary), Use of Alternate Decay Heat Removal in Mode 6 Refueling dated January 2003," WOG-03-254, May 12, 2003.

By letter dated October 2, 2003, the Nuclear Regulatory Commission (NRC) issued a Request for Additional Information (RAI) for WCAP-15872-NP, "Use of Alternate Decay Heat Removal in Mode 6 Refueling," (Ref. 1). Westinghouse Electric Company LLC (Westinghouse) on behalf of the Westinghouse Owners Group (WOG) submitted WCAP-15872-NP for approval in May 2003, (Ref. 2).

The purpose of this letter is to transmit responses to the staff RAIs (Enclosure 1). In addition, changes were required to portions of WCAP-15872 to be consistent with these RAI responses. These changed pages are provided in Enclosure 2. All updated pages will be integrated into the final approved version of WCAP-15872-NP.

D048

Information transmitted by this letter is non-proprietary and may be released to the public. If you require further information, please contact Mr. Jim Molkenthin in the Owners Group Program Management Office at (860) 731-6727.

Sincerely yours,

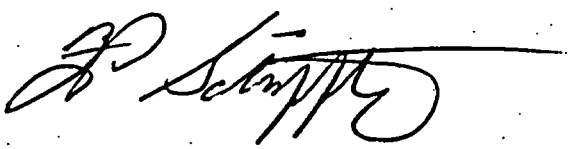

Frederick P. "Ted" Schiffley, II
Chairman
Westinghouse Owners Group

Enclosures: (2)

cc: S. Dembek, NRC, Westinghouse
D. G. Holland, NRC (via Federal Express)
Management Committee
Steering Committee
Analysis Subcommittee
Project Management Office
C. B. Brinkman, Westinghouse
J. S. Galembush, Westinghouse
V. A. Paggen, Westinghouse

Enclosure 1

WCAP-15872, "Use of Alternate Decay Heat Removal in Mode 6 Refueling"

RAI Responses

WCAP-15872-NP, R00
"Use of Alternate Decay Heat Removal in Mode 6 Refueling"
Request for Additional Information
dated October 2, 2003

Main Report

RAI 1. What is a shutdown cooling "train?" Describe the physical setting of the two "trains" mentioned in Sec 2.2 of the text when they are inoperable at the time of the initiation of the alternate heat removal alignment, and when they are supplementing the shutdown cooling system.

Response:
A shutdown cooling (SDC) train is a dedicated flow path consisting of piping, valves, a low pressure safety injection pump and a SDC heat exchanger that provides cooling of the reactor core during shutdown conditions in Modes 4, 5 & 6. Two such shutdown cooling trains constitute the shutdown cooling system installed at licensed plants. A brief description of the shutdown cooling system and the alternate cooling alignment for removing decay heat from the refueling pool during Mode 6 operation is given in Sections 2.1 and 2.2, respectively, of WCAP-15872.

Standard Technical Specifications, e.g., NUREG-1432, LCO 3.9.4, require that one of the two SDC system trains be operable and in operation during Mode 6 conditions with the refueling pool fully flooded. The alternate heat removal (AHR) alignment will function as a complete substitute for the SDC system, thereby permitting the shutdown cooling system to be taken out of service once decay heat removal using the alternate cooling alignment is placed in service. Thereby, AHR promotes outage schedule flexibility when maintaining plant equipment during Mode 6 operations.

The reference to supplementing the SDC system refers to the opportunity for a utility to ensure decay heat removal by having AHR capability available to support normal SDC, either in combination with an operable SDC train, or as stand-by should normal SDC become inoperable.

RAI 2. Is your methodology predicated on the use of the spent fuel pool cooling system as the alternate heat removal system?

Response:
The alternate heat removal system is predicated on use of any appropriate and available cooling system that has adequate heat removal capability, can be aligned to remove heat from the refueling pool, and is judged to be sufficiently reliable. In WCAP-15872, the alternate heat removal alignment is modeled after that of Calvert Cliffs, where a spent fuel pool cooling train can be used as the alternate system to receive decay heat in Mode 6 with the refueling pool fully flooded.

Appendix A: Algorithm for Natural Convection between Core and Refueling Pool

For the one-dimensional model of the core and refueling pool:

RAI A1. Superimpose the nodalization that your methodology assumes on Fig. A-1. Demonstrate that it is robust.

Response:
The analysis is based on division of the refueling pool and reactor vessel internals into a series of control volumes. The state points for these one-dimensional control volumes are shown in Figure A-1 and identified as follows:

1 = Reactor vessel inlet at the level of the vessel flange.
2 = Core inlet at the level of the fuel alignment plate.
3 = Reactor vessel lower plenum at the bottom of the core.
4 = Core exit at the level of the fuel alignment plate.
5 = Reactor vessel exit at the level of the vessel flange.
6 = Bulk refueling pool.
7 = Alternate cooling inlet to pool.
8 = Alternate cooling exit from pool.
9 = Shutdown cooling inlet.
10 = Shutdown cooling exit.

These state points represent natural boundaries between the control volumes and are consistent with the set of assumptions used to reduce the refueling pool coupled circulation problem to tractable form. The robustness of this model is demonstrated by its close agreement with the test data obtained at Calvert Cliffs.

RAI A2. What are the assumed mass, momentum and energy equations for the related control volumes?

Response:
The one-dimensional model is based on the following general control volume formulations for conservation of mass, momentum and energy:

Conservation of mass,

$$\frac{\partial}{\partial t}\int_{cv}\rho dV+\int_{cs}\rho\vec{v}\cdot d\vec{A}=0$$

Conservation of energy,

$$\dot{Q}_{CV}-\dot{W}_{CV}-\dot{W}_{SHEAR}+\int_{cv}q'''dV=\frac{\partial}{\partial t}\int_{cv}e\rho dV+\int_{cs}\left(e+\frac{p}{\rho}\right)\rho\vec{v}\cdot d\vec{A}$$

Conservation of momentum,

$$\sum_{CV} \vec{F} = \vec{F}_S + \vec{F}_B = \frac{\partial}{\partial t}\int_{CV} \vec{v}\rho\, dV + \int_{CS} \vec{v}\,\rho\vec{v}\cdot d\vec{A}$$

where W_{CV} is mechanical work, W_{shear} is work done by shear and $\dot{Q}_{CV}$ is the heat generation within the control volume.

These equations, based on the following assumptions and expressed in finite difference form, are solved using the algorithm shown in Figure A-2.

Assumptions involving flow through the core:

- Upper guide structure and fuel alignment plate have been removed.
- One-dimensional, steady-state flow with no horizontal cross-flow for vertical flow paths.
- Neglect changes in kinetic and potential energies of the water flowing through the core.
- Neglect any ambient heat loss, $\dot{Q}_{loss} = 0$.
- Heat generation is constant and uniformly distributed throughout the core control volume, $\int_{CV} q'''\, dV = \dot{Q}_{CV}$
- Work associated with rotating shafts and moving boundaries is zero, $\dot{W}_{CV} = 0$.
- Work due to shear stress is negligible, and shear stress on the surface of the control volume is uniformly distributed, $\tau \neq \tau(z)$.
- Temperature increases with depth for down flow path, $T_2 < T_3$ so that $\rho_2 > \rho_3$.
- Density varies linearly with elevation, $\rho = \rho_2 - \Delta\rho\frac{(z_2 - z)}{L}$, where $\Delta\rho = \rho_2 - \rho_3$, and $L = z_2 - z_3$.
- No heat storage in the fuel.
- The upflow and down flow areas are identical, $A_2 = A_3 = \frac{A_{core}}{2} \equiv A_{1/2\,core}$.
- Heat generation in the core control volume results in an increase in temperature, so that $\frac{\partial}{\partial t}\int_{CV} e\rho\, dV \neq 0$.

Refueling Pool: assumptions:

- One-dimensional, steady-state flow along a streamline.
- Change of momentum within CV, $\frac{\partial}{\partial t}\left[\int_{CV} \vec{V}(\rho dV)\right] = 0$.
- Frictionless flow, i.e., no viscous losses.

- Heat transfer from the pool surface due to natural convection and evaporation, $\dot{Q}_{CV} = -\left[h_{\infty} A_{surf}(T_6 - T_{amb}) + \dot{m}_{evap} h_{fg}\right]$.
- Neglect kinetic and potential energy changes of the water flowing through the pool. Neglect work due to shear.
- A fraction of the pool water, e_{mix}, mixes with the core flow.

For one-dimensional flow through the core, shown as flow path 3 – 4 on Figure A-1:
Conservation of mass:

$$\dot{m}_3 = \dot{m}_4 = \rho_3 A_3 v_3 = \rho_4 A_4 v_4$$

Conservation of energy:

$$p_3/\rho_3 + v_3^2/2 + gz_3 = p_4/\rho_4 + v_4^2/2 + gz_4 + K_{34}\bar{v}^2/2$$

Conservation of momentum:

$$-p_4 A_4 + p_3 A_3 - \tau_{34} A_{surf34} - g\frac{\rho_3 + \rho_4}{2} A_{1/2core} L_{core} = \dot{m}_4 v_4 - \dot{m}_3 v_3$$

For one-dimensional flow through the pool:
Conservation of mass:

$$\dot{m}_5 = \dot{m}_6 = \rho_5 A_5 v_5 = \rho_6 A_6 v_6$$

Conservation of energy:

$$\varepsilon_{MIX} M_{pool} c_p \frac{d\bar{T}_6}{dt} + \dot{Q}_{surf} = \dot{m}_{core} c_p (T_5 - T_1) - \dot{m}_7 c_p (T_8 - T_7)$$

Conservation of momentum:

$$\frac{p_5}{\rho_5} + \frac{v_5^2}{2} + gz_5 = \frac{p_6}{\rho_6} + \frac{v_6^2}{2} + gz_6$$

The fraction of the alternate heat removal cooling flow that does not mix with the thermal plume is expressed by the bypass coefficient, e_{bypass}. Thus, the refueling pool exit temperature, T_8, can be expressed in terms of the bypass coefficient, the pool average temperature, T_6, and the alternate heat removal inlet temperature, T_7, as:

$$T_8 = (1 - e_{bypass})T_6 + e_{bypass}(T_7)$$

When the bypass coefficient is zero, all alternate heat removal cooling flow mixes with the thermal plume, or T_8 equals T_6. If none of the alternate cooling flow mixes with the thermal plume, then e_{bypass} equals one and the pool exit temperature T_8 equals T_7.

RAI A3. What is meant by "The effective mass is determined by engineering judgment?" How is the numerical value for use in the one-dimensional model computed?

Response:
The effective mass, defined as e_{mix} times the pool mass, identifies the quantity of fluid in the refueling pool that mixes with the natural convection flow from the core. This mass is

determined through CFD analysis when solving for the mixing coefficient. Engineering judgment refers to the review to ensure that predicted results are verified by test data.

RAI A4. What results show that the mixing coefficient $\dot{\epsilon}_{mix}$ is about 0.90? What are the parameters to which the value of $\dot{\epsilon}_{mix}$ is most sensitive? What is the sensitivity of $\dot{\epsilon}_{mix}$ to these parameters?

Response:
The mixing coefficient is described in terms of the initial pool temperature and the pool average temperatures from one-dimensional and CFD computations. Since the mixing coefficient influences the rate of temperature change in the one-dimensional model, it was necessary to use a transient CFD case to evaluate e_{mix}. For a refueling water pool cooling configuration typical of CCNPP but having no alternate cooling flow, the mixing coefficient was evaluated based on the time required for the average pool temperature to reach saturation as determined by the CFD model. Table D-3 illustrates the time required to reach the boiling point for three different pool elevations and the associated mixing coefficient as predicted by the CFD model. Based on this data, a mixing coefficient of 0.9 was selected as the best representative value for use in one-dimensional analyses.

The principal parameters affecting the mixing coefficient are the refueling pool cooling configuration and the mass flow rate driven by natural circulation between the core and the refueling pool. No alternate heat removal cooling flow was assumed when computing the mixing coefficients given above, which ensures conservative results for all alternate heat removal cooling configurations. In addition, parametric evaluations using the one-dimensional model based on arbitrary variations of the mixing coefficient did not produce significant variations in pool temperature or core flow rate.

With regard to the sensitivity of these parameters, based on the alternate heat removal conditions at Calvert Cliffs, an arbitrary reduction in core flow rate of 20% resulted in about a 10% reduction in the mixing coefficient. Also, for the same core flow rate, the mixing coefficient was found to vary approximately ± 5% when based on average temperatures at specific locations rather the entire refueling pool.

A typographical error was found in Table D-3. The temperatures shown in the column labeled "Bottom" should read 874°F, 212°F and 215.5°F, respectively. The CFD value for e_{mix} should be 1.03, while the one-dimensional value for e_{mix} is 1.0. Table D-3 has been revised to show these corrected values.

RAI A5. How is the value of the by-pass fraction $\dot{\epsilon}_{bypass}$ computed? What "results show" that $\dot{\epsilon}_{bypass}$ is close to 1.0? How close? What is the sensitivity of $\dot{\epsilon}_{bypass}$ to key parameters?

Response:
The by-pass coefficient is defined in terms of mass flow rates and is computed using the expression for e_{bypass} shown in Section D-2. Mass flow rates, in turn, are determined from pool temperatures predicted by the CFD model. For the Calvert Cliffs configuration modeled in this analysis and represented by Configuration A in Table D-2, results demonstrate that the value of

the bypass coefficient is approximately zero for alternate heat removal cooling flow rates varied from 200 to 2000 gpm.

Table D-2 also shows that the value of the bypass flow coefficient depends strongly on the refueling pool configuration, specifically the relative locations of the inlet and outlet for the alternative cooling flow. Comparing configurations A and B, it is seen that a factor of ten difference in alternate cooling flow rate has a minor impact on the bypass coefficient when the coolant flow interacts with the natural convection plume from the reactor core, whereas configurations with the inlet and outlet on the same side of the pool have significant differences in the bypass coefficient. A similar result is seen when comparing configurations C and D, although computations indicate substantial entrainment of the pool water by the alternate cooling flow occurs for large flow rates in configuration C.

RAI A6. Are $\dot{\epsilon}_{bypass}$ (in the equations) and β (Table A-1) the same coefficient?

Response:
The terms e_{bypass}, ß, and $ß_{bypass}$ as used in WCAP-15872 Rev 00 are the same coefficient. For consistency, the term "e_{bypass}" is used to define the bypass coefficient in these RAI responses and in any revisions made to WCAP-15872.

RAI A7. Please show the derivation of the values of $\dot{\epsilon}_{mix}$ and $\dot{\epsilon}_{bypass}$ used in the results shown in Figs. A-3 and A-4 for Case 2 and Case 3.

Response:
The mixing and bypass coefficients are defined in Appendix A and derived as shown in Appendix D. However, for the results shown in Figure A-3 and Figure A-4, these coefficients were assumed well mixed, i.e., e_{mix} =1.0 and all alternate heat removal flow fully mixed with the natural convection flow from the core, e_{bypass} = 0.0. In Appendix A, Case 2 represents full SDC flow plus alternate cooling flow; Case 3 represents only alternate cooling flow. (Note that sample Cases 1 – 4 in Appendix A are not the same as test Cases 1 – 4 listed in Appendices B, C and D.)

Appendix B: Comparison of Predictions with Test Data

RAI B1. Fig. B-1 is confusing. Under the alternate cooling alignment do you have a separate spent fuel pool (SFP) pump and heat exchanger for both the refueling pool and the SFP, or do these represent separate alignments? Please indicate the complete flow paths of fluid associated both with the refueling pool and core, and the SFP. In your figure, how and when do you get flow "from the refueling pool to the spent fuel pool?"

Response:
Figure B-1 illustrates the specific alternate heat removal alignment at CCNPP. The figure describes the capability to align a "spare" spent fuel pool cooling train to cool the refueling pool while a second train remains aligned to the site's spent fuel pool.

The complete alternate heat removal process fluid flow path at Calvert Cliffs is where heat from the core exchanges with the refueling pool through natural convection, then forced flow from the

pool through a train of the spent fuel pool cooling system (pump, heat exchanger and piping). The discharge from this alternate cooling alignment flow path is then returned to the refueling pool.

The statement in Section B.1, "The suction from the refueling pool to the spent fuel pool cooling line is through a drain in the bottom of the refueling pool, at the side of the pool opposite the inlet point," refers to the alternate heat removal alignment at Calvert Cliffs. In this alignment, major components (pump, heat exchanger, piping) from one train of the spent fuel pool cooling system are cross-connected to suction and discharge fittings in the Calvert Cliffs refueling pool. A direct exchange of coolant between the spent fuel pool and the refueling pool is not relied upon to support the alternate heat removal process.

The actual configuration of the alternate cooling alignment implemented at other plants may vary depending upon the available plant equipment capabilities. Refer also to Figure 1 of WCAP-15872 which illustrates a generic shutdown cooling decay heat removal system, and to Figure 2 which illustrates the decay heat removal flow path when using the Alternate Heat Removal process. A different alternate heat removal alignment may be selected by other plants, depending on the heat removal loops available to cool the refueling pool. The alternate heat removal process does not envision altering the traditional method of cooling the spent fuel pool.

RAI B2. In Table B-1, what is "SW?"

Response:
The term "SW" refers to Service Water. This term is included in an updated acronym list for WCAP-15872.

RAI B3. You report average temperatures. These are averaged over what?

Response:
Temperatures given in Table B-1 are averaged over times recorded for the tests.

RAI B4. Table B-2, B-3 and B-4 report time in days, hours and minutes respectively. Also, the figures use two different time scales. Please resubmit for review all tables and figures based on one time scale. (If there is a specific reason, such as clarifying a relationship, state so.)

Response:
Time scales in Tables B-2, B-3 and B-4 are expressed in terms of clock time, total elapsed time and time in days after shutdown in order to expediently illustrate a particular result. For example, an event having a duration of minutes is not easily illustrated if expressed using a time-scale of days. Total elapsed time is used to compare measured and predicted values, while days after shutdown is the important parameter for tracking the point at which changes such as initiation and securing of shutdown cooling, head removal, initiation and securing of alternate cooling, and return to shutdown cooling occur.

RAI B5. Please give a table describing the physical conditions associated with each of the five cases. That is, for each of the five cases, give the initial and final time and the corresponding initial, final and average shutdown cooling and SFP temperatures (computed and measured), flows and core decay powers. For average values, give the explicit method by which they were computed.

Response:
The physical conditions, time, and temperatures associated with the test cases listed in Table B-3 are given below. The reactor is in Mode 6 with the refueling pool fully flooded for Cases 2 - 5.

Case 1: SDC flow reduced while the reactor vessel head is removed.
Case 2: SDC flow restored to value prior to head removal.
Case 3: AHR flow initiated, SDC flow continued.
Case 4: SDC flow secured, AHR cooling only.
Case 5: SDC flow restored, AHR flow secured.

Case	Event Date and Time	DAS (Days)	Analysis Time		Temperature (°F)				
			Start-hr	End-hr	SDC-in	SDC-out	AHR-in	AHR-out	RFP
1	03/23/01, 04:30	5.75	0	11	73.58	102.90	NA	NA	NR
2	0323/01, 15:30	6.21	11	285	92.01	102.73	NA	NA	NR
3	04/03/01, 22:00	17.62	285	298	99.00	103.30	92.03	96.78	101.30
4	04/04/01, 13:00	18.21	298	348	NA	NA	78.16	92.95	99.26
5	04/07/01, 13:40	20.49	348	375	96.72	102.89	NA	NA	NR

The purpose of Table B-3 is to document measured temperatures with their corresponding times. Table B-4 lists the analysis times used for predictions corresponding to Cases 1 - 4 in Table B-3.

Time histories of the data for each of these cases are documented in Figures B-3 (SDC flow and temperatures), B-4 (AHR temperatures and flow rate) and Figure B-5 (RFP temperatures). Predictions for Cases 2, 3 and 4 are shown in Figure B-6.

Appendix C: Comparison of CCNPP Unit 2 Test Data with Computational Fluid Dynamics (CFD) Predictions

RAI C1. For these calculations, please show the natural circulation flow path in the core region. Is that how is the core cooled?

Response:
Decay heat is transferred from the core to the refueling pool through natural circulation. While this heat removal is not dependent on the direction of the circulatory pattern through the core, good agreement between fluid temperatures based on the CFD analysis and the Calvert Cliffs test data at the reactor vessel flange elevation was predicted assuming a natural circulation path with down-flow in the center of the core and up-flow at the core periphery. This flow pattern was found to best represent the post-refueled conditions, where fresh fuel occupies a checkerboard arrangement in the core center, which existed during the alternate heat removal test phase at Calvert Cliffs.

RAI C2. The results from the lumped parameter model (core flow rate) are dependent on $\dot{\epsilon}_{mix}$ and $\dot{\epsilon}_{bypass}$. These two coefficients are determined via a CFD calculation. How does the CFD calculation of $\dot{\epsilon}_{mix}$ and $\dot{\epsilon}_{bypass}$ differ from the CFD calculation in this appendix?

Response:
The CFD evaluations of Appendices C and D are based on parameters for the CCNPP refueling pool/reactor cavity geometry. Appendix C contains an evaluation of the specific flow and temperature fields associated with the CCNPP flow alignment (similar to Configuration A of Appendix D) at the initial and boundary conditions associated with the CCNPP Unit 2 test data. Appendix D contains the evaluation of the heat removal capabilities of permissible flow alignments and includes the evaluation of the mixing and bypasses coefficients for each alignment. As such, Appendix C represents a validation of the CFD computations and the application of the mixing and bypass coefficients from Appendix D into the lumped parameter model which computes the core flow rate. Small changes in the initial and boundary conditions associated with the CCNPP2 test data, including a lower alternate cooling flow rate, do not substantially alter the computed mixing and bypass coefficients presented in Appendix D. Thus, the methods used to calculate the mixing and bypass coefficients given in Appendix C are the same as those for the remainder of WCAP-15872.

RAI C3. Is the CFD calculation in this appendix a steady-state calculation?

Response:
The CFD computations are steady state based on the observation that the refueling pool is in a quasi-steady state condition for the purposes of Appendix C.

RAI C4. The data appear to show no temperature gradient at the flange level, while the CFD calculation shows a distinct gradient. Your proffered explanation in paragraph eight is not clear. Please provide a drawing indicating the flows and temperatures that support your argument.

Response:
The application of a rectangular Cartesian grid to represent a cylindrical reactor vessel cavity accentuates local temperature differences when comparing CFD temperature predictions with thermocouple data at the flange level. Pool temperature data from CCNPP Unit 2 were taken in four strings starting just above the reactor vessel flange; these thermocouples are radially near, but not necessarily in, the rising thermal plume. The corner cells just above the reactor cavity and within the computed thermal plume are the closest representations in the CFD model to these thermocouple locations. As a consequence, the average temperature of the four computational cells would be expected to be higher than the average of the test data. This rationale is confirmed in Table C-1 where the average CFD temperature exceeds the data by only 3.6°F at the 44-ft elevation. The average temperatures are much closer at the mid-pool and pool-surface elevations since the CFD model can better represent the global turbulent diffusion and convective diffusion.

The horizontal temperature gradients at the flange level are more pronounced as a consequence of the rectangular grid approximation to the circular reactor cavity opening at the flange. The rectangular grid causes a more pronounced channeling of pool currents around the

flange opening than might be expected from currents around a circular flange opening. As shown in Figure C-6, the channeling of current is evident as longer velocity vectors passing one side of the flange opening in the velocity distribution of the horizontal plane just above the flange. In turn, the enhanced channeling promotes a somewhat larger temperature difference between opposite sides of the flange, as evident in the temperature distribution in the horizontal plane just above the flange and seen in Figure C-3.

Both of these effects are localized at the reactor cavity opening. The turbulent thermal diffusion and convective diffusion of the thermal plume into the bulk refueling pool are otherwise well represented and indicated by the good agreement in temperatures at higher elevations.

RAI C5. How is the difference in mixing, described in C4 above, taken into account in your estimate of $\dot{\epsilon}_{mix}$?

Response:
The pool mixing coefficient is defined in terms of pool average temperatures. The impact of localized currents is accurately represented in the global mixing although the localized temperature results may not precisely correlate with the CCNPP data in the flange area.

Appendix D: Evaluation of Alternative Heat Removal Alignments

The key to your methodology is the estimation and validation of the mixing and bypass coefficients. Please define your terminology clearly; indicate the type of calculation and the results precisely so that the comparisons are clear.

RAI D1. Please describe the simplified one-dimensional computational model and its relation to the two-dimensional computational fluid dynamics model. How does it differ from the one-dimensional model discussed in Appendix A? When you say "computational fluid dynamics model" (without the adjective "one-dimensional") in D.3, what are you referring to - A 3D model? Figures D-3 through D-6 give 2D results. So, how are you treating the situation in Figure D-2?

Response:
The mixing and bypass coefficients reflect three-dimensional effects into the one-dimensional analysis, shown in Appendix A, for natural circulation flow rates and refueling pool temperatures. The mixing coefficient is a measure of the uniformity of the refueling pool temperature, while the bypass coefficient, represented schematically in Figure D-2, is an indicator of the flow rate from the alternate cooling alignment that bypasses the natural circulation plume from the core.

Predictions of refueling pool temperatures using the three-dimensional CFD model, described in Appendix C, are then used to calculate both mixing and bypass coefficients. These values are then used in the one-dimensional model. Final values are selected based on agreement between the one-dimensional predictions, the CFD analysis results, and the data.

RAI D2. You say "The one-dimensional evaluations based on perfect mixing ... are summarized in Table D-2," yet you show bypass flows that are not one-dimensional.

In Table D-3 what is your point? The table indicates that the mixing coefficient is spatially dependent (given at different locations). How can that be when it is defined on page D3 in terms of pool average temperatures?

Response:
The statement referring to perfect mixing (e_{mix} = 1.0) and all alternate cooling flow passing over the core (e_{bypass} = 0.0) are assumptions used in the one-dimensional scoping analysis shown in Appendix A.

The mixing coefficient is defined in Appendix D in terms of the initial pool temperature and the pool average temperatures from one-dimensional and CFD computations. A number of CFD cases were run to evaluate the range of the mixing coefficient since the mixing coefficient influences the rate of pool temperature change in the one-dimensional model. Results for the case selected to best represent the mixing coefficient are reported in Table D-3. In that table, a one-dimensional model with the mixing coefficient set equal to 1.0 establishes a time, 886 minutes, when the pool average temperature reaches saturation. By interpolation, the equivalent time predicted by the CFD model to achieve a pool average temperature of saturation is 851 minutes, which reasonably agrees with the one-dimensional prediction. Results of the CFD model at other times, which correspond to reaching the saturation temperature at an elevation representing the core exit, the free surface, and the bottom of the refueling pool are also shown in the table. For these locations, the mixing coefficient was found to be 0.88, 0.98, and 1.03, respectively, from which a representative value of 0.90 was selected for use in one-dimensional analyses.

Appendix E: CCNPP Specific Evaluation of Conditions for Alternate Decay Heat Removal in Mode 6

RAI E1. In section E.1, your discussion of Figure E-3 is inconsistent with the text. The text indicates that the initial refueling pool temperature is 75°F, while the value in the figure at t = 0 is 90°F.

Response:
The initial temperature of the refueling pool was taken as 90°F in the analysis. Page E3 of Appendix E has been corrected to be consistent with Figure E-3.

RAI E2. Where are the data that reflect the last statement on page E3? What is the basis for the "expected" high and low limits?

Response:
The statement concerning expected high and low limits is not needed and has been deleted.

RAI E3. What is the purpose of footnote 1 on page E4? Where and what is Reference 6.1?

Response:
The footnote was meant to reference standard methods used to determine heat exchanger effectiveness and outlet temperatures. This footnote and reference are not needed and have been deleted.

RAI E4. In the paragraph Limiting THS vs. TAS on page E4, Figure E-5 does not show a family of curves. What do you mean by a 90°F heat sink temperature when the refueling pool inlet temperature in also 90°F?

Response:
The statement has been corrected to refer to Figure E-4, not E-5. Figure E-5 is a cross-plot of the data shown on Figure E-4. The heat sink statement refers to the temperature of the heat sink for heat removal, which in this case is the inlet temperature to the spent fuel pool heat exchanger.

RAI E5. The time scale of minutes on the x-axis of the figures is inappropriate for the phenomena described on the figure. Please submit a revised figure that uses a consistent time scale (see Appendix B, Question B4).

Response:
The different time scales reflects differences in the information represented in the figures. For example, Figures E-1, E-3, E-5 and E-7 reflect the influence on the days after shutdown on the value of decay heat assumed in the subsequent analyses. Figures E-2, E-4 and E-6, reflect the time, the order of magnitude being minutes, for the refueling pool temperature to reach a new steady state value after the noted changes in operating conditions. Thus, the time scales selected are appropriate to the information represented and do not warrant changes to the report.

RAI E6. What is Reference 6.4 which gives the CFD analysis that establishes the maximum fluid velocity for the computation of the force on the fuel assembly?

Response:
The reference was for the CFD analysis and is not needed. This reference has been deleted.

RAI E7. How do you get from a one-dimensional model the flow rate in the core for a lateral velocity of 0.22ft/sec in the refueling pool? The precision is astounding!

Response:
The velocities were taken from the CFD analysis and are representative of the magnitude of lateral velocities that could be expected. The text has been revised to state that the velocity is approximately 0.2 ft/sec.

Enclosure 2

WCAP-15872, "Use of Alternate Decay Heat Removal in Mode 6 Refueling"

Changed Pages

WCAP-15872-NP
Use of Alternate Decay Heat Removal in Mode 6 Refueling

List of Changed Pages

Report Body:
- Pg ii (List of Acronyms)

Appendix A
- Pgs A2 – A8
- Pg A13
- Pg A14

Appendix B
- Pgs B2 - B5
- Pg B10
- Pg B11

Appendix C
- Pgs C2 - C4

Appendix D
- Pgs D2 – D6
- Pg D8

Appendix E
- Pgs E2 – E6
- Pgs E14 – E16

List of ACRONYMS

AHR.....Alternate Heat Removal
CCNPP..... Calvert Cliffs Nuclear Power Plant
CCW .....Component Cooling Water
CDF.....Core Damage Frequency
CFD.....Computational Fluid Dynamics
DAS.....Days after Shutdown
DHR ..... Decay Heat Removal
EOP.....Emergency Operating Procedure
FPCS.....Fuel Pool Cooling System
gpm .....Gallons per Minute
HPSI.....High Pressure Safety Injection
HX ..... Heat Exchanger
LCO.....Limiting Condition for Operation
LOCA ..... Loss of Coolant Accident
LPSI .....Low Pressure Safety Injection
MEEL ..... Minimum Essential Equipment List
NPSH ..... Net Positive Suction Head
NRC .....Nuclear Regulatory Commission
RCS..... Reactor Coolant System
RFP..... Refueling Pool
RV ..... Reactor Vessel
SDC.....Shutdown Cooling System
SFP .....Spent Fuel Pool
SW ..... Service Water
T_{amb} .....Containment ambient temperature
TAS .....Time after Shutdown
T_{HS}, THS.....Heat Sink Temperature
TRM .....Technical Requirements Manual
TS ..... Technical Specifications
UGS .....Upper Guide Structure
ε_{mix}, ε..... Ratio of mixed RFP mass to total RFP mass
ε_{bypass}, ß, $ß_{bypass}$ ..... Ratio of AHR flow bypassing core to total AHR flow

APPENDIX A

ALGORITHM FOR NATURAL CONVECTION BETWEEN CORE AND REFUELING POOL

APPENDIX A
ALGORITHM FOR NATURAL CONVECTION BETWEEN CORE AND REFUELING POOL

A.1 MODEL

In Modes 5 and 6, forced convection provided by the shutdown cooling system is used to transport decay heat from the reactor core to the ultimate heat sink. In the absence of shutdown cooling flow during Mode 6 refueling operations with the refueling pool flooded, the reactor core decay heat is transported by natural circulation into the refueling pool water. The buoyancy force causing this natural circulation is driven by the density difference between the cooler, denser, fluid in the refueling pool and the hotter, less dense, flow through the core. Interaction between the natural circulation flow through the core with the circulating currents in the refueling pool results in a variation of fluid temperatures and velocities within the refueling pool. Properties controlling the natural convection from the reactor to the refueling pool as well as natural convection and evaporation from the free surface are primarily functions of temperature.

The model described in this Appendix has been developed to calculate the natural convection flow between the core and refueling pool that occurs during Mode 6 refueling conditions when the shutdown cooling system is not in operation. This model divides the reactor vessel and refueling pool into a series of control volumes that describe the upper guide structure, core and refueling pool, Figure A-1. Mass flow rates and inlet temperatures are prescribed for the alternate heat removal flow path. Conservation of mass, momentum and energy for these control volumes are solved to predict the mass flow rate between the reactor vessel and refueling pool. Temperatures are calculated for the refueling pool, the flow into and out of the pool, and the flow rate through the alternate heat removal alignment. The model also considers the heat lost at the pool surface due to natural convection and evaporation from the free surface. Dependent and independent variables are defined in Table A-1.

The flows into and out of the control volumes are assumed one-dimensional. However, the natural convection flow being driven by the temperature difference between the core and refueling pool is allowed to vary with time. This heat storage is accounted for in the mass of coolant in the pool as well as the coolant and structural masses for the upper guide structure and the core. Without active heat removal provided by the alternate heat removal alignment, the temperature of the refueling pool would continue to increase until the boiling point is reached. With active heat removal, steady state temperatures are eventually reached for core, pool and outlet flow.

The geometry of the pool results in regions where the cooler fluid near the bottom of the pool does not fully mix with the core flow. This is modeled by defining a mixing coefficient, ε_{mix}, which is defined as the ratio of the effective mass of coolant in the refueling pool that mixes with the reactor vessel flow to the total mass of coolant in the refueling pool. Therefore, the mixing coefficient is the effective fraction of the pool water that participates in the core-to-pool flow process.

$$\varepsilon_{mix} = M/M_{refueling\ pool}$$

The effective mass is determined by engineering judgment from the temperature and velocity distributions in the computational fluid dynamics model used to address the

refueling pool. The flows between the core and the fraction of the mass of fluid in the refueling pool, defined by the value ε_{mix}, which participates in the fluid transfer, are assumed to be fully mixed. Analysis shows the majority of the refueling pool inventory mixes with the natural convection flow from the core, resulting in a value for the mixing coefficient of about 0.90.

In addition, not all the flow from the alternate cooling path mixes with the natural convection driven flow from the core. This is accounted for by defining a bypass fraction, defined as the ratio of the flow bypassing the core plume flow to the total pumped alternate heat removal flow, or:

$$\varepsilon_{bypass} = m_{bypass\ flow} / m_{AHR\ flow}$$

The value of the bypass coefficient is determined from the computational fluid dynamics model. Analysis shows that essentially all of the alternate heat removal cooling flow injected into the refueling pool mixes with the natural circulation plume above the vessel, resulting in a bypass coefficient close to zero.

A.2 Algorithm

The solution algorithm solves for the core exit temperature, T_4, and the pool temperature, T_6, for each time step, $t_{n+1} = t_n + \Delta t$. The algorithm iterates on core exit temperature at each time step, with the following basic steps;

- Select Q_{core}
- Assume $T_4 (\equiv T_{out\ of\ core}) > T_6 (\equiv T_{pool} \equiv T_{Into\ core}) = T_1$
- Solve for $\rho\ (T_4)$
- Solve for $\dot{m}_{core}$
- Solve for new $T_4 (\equiv T_{new\ out\ of\ core,\ new})$
- Iterate until $T_{core\ new}$ minus $T_{core\ old}$ is within the convergence criteria (0.10°F)
- Solve for new pool temperature, $T_{6,\ new}$

This algorithm, Figure A-2, is evaluated for each time step until a steady state or until the saturation temperature is reached, $T_4 = T_{core\ new} = T_{sat}$.

Values for the independent variables for CCNPP Units 1 or 2 are listed in Table A-2. Sample cases for four combinations of shutdown cooling and alternate heat removal flow are listed in Table A-3. The upper guide structure has been removed in all cases. Thus, values of structural mass and loss factors for the upper guide structure are taken as zero. Selection of values for the time step (15 seconds) and convergence criteria (0.10°F) are based on a convergence study. Output parameters are defined in Table A-4. Sample results are shown in Table A-5.

Results for average refueling pool temperatures and natural circulation flow are shown in Figures A-3 and A-4. Case 1 represents normal alignment for active shutdown cooling. In Case 2, both the alternate heat removal and shutdown cooling are active, resulting in the lowest values of refueling pool temperature. Case 3 is for alternate heat removal alone. The refueling pool temperatures remain below saturation in all cases. Case 4, with both shutdown cooling and alternate heat removal flow secured, represents the condition for no active cooling of the refueling pool.

With shutdown cooling flow in operation, the flow rate between the core and refueling pool due to natural circulation is approximately 2000 gpm; with shutdown cooling flow secured this natural circulation flow rate increases to approximately 4000 gpm as shown on Figure A-4. These flow rates are driven by the temperature difference between the core and refueling pool. Cases 1 and 2, where shutdown cooling is active, have lower flows and lower temperature differences. Case 4, with no forced cooling flow, has the largest natural circulation flow through the core and the largest values of temperature difference.

Table A-1
Definition of Variables

ANALYSIS	DEFINITION	QBASIC	UNITS
T_1	UGS inlet temperature	T_{pnew}	°F
T_2	Core inlet temperature	T_{pnew}	°F
T_4	Core outlet temperature	T_{cnew}	°F
T_5	UGS outlet temperature	T_{cnew}	°F
T_6	Refueling pool temperature	T_p	°F
T_7	SFP flow inlet temperature	T_{pin}	°F
T_8	SFP flow outlet temperature	T_{pout}	°F
T_9	SDC flow inlet temperature	T_{sdcin}	°F
T_{10}	SDC flow outlet temperature	T_{cnew}	°F
m_{core}	Core flow due to natural convection	m_{core}	lbm/sec
m_7	SFP flow rate	m_{pdot}	lbm/sec
m_{sdc}	SDC flow rate	m_{sdc}	lbm/sec
M_{24}	Mass of water & metal in the core	M_{cf} ,M_{cm}	lbm
M_{16}	Mass of water & metal in the UGS	M_{ugsf} M_{ugsm}	lbm
M_6	Mass of water in the refueling pool	M_p	lbm
P_{amb}	Containment pressure	P_c	psia
T_{amb}	Containment temperature	T_c	°F
Q_{fuel}	Decay heat	Q_c	btu/sec
Q_{surf}	Heat loss at pool surface due to natural convection and evaporation	$Q_{pnc+pevap}$	btu/sec
Δt	Time step	Δt	sec
ε_{bypass}	Alternate heat removal cooling flow bypass coefficient	ε_{bypass}	Note 1
ε_{mix}	Refueling pool mixing coefficient	ε_{mix}	Note 2

Notes:

1 No bypass = 0, all bypassed = 1
2 No mixing = 0, complete mixing = 1

Table A-2
Input for CCNPP Units 1 & 2

COMPONENT	PARAMETER	SYMBOL	VALUE	UNITS	NOTES
Containment	Pressure	P_{amb}	14.7	psia	1
	Ambient Temp	T_{amb}	75	°F	1
Refueling Pool	Water mass	Mf1	3084708	lbm	
	Water depth	L1	23	ft	
	Free surface	A_{surf}	1750	ft^2	
	Wetted Perimeter	P_{wet}	190	ft	
	Equiv Length	L_{eq}	9.21	ft	2
	SFP flow rate	Q_{sfp}	-	gpm	Case dependent
	SFP inlet Temp	T_{sfpin}	-	°F	Case dependent
	Mixing Coefficient	$0 < \varepsilon_{mix} \leq 1$	0.90	-	
	Natural Conv		> 0	-	> 0 = yes
	Evaporation		> 0	-	>0 = yes
	Bypass Coefficient	$0 < \varepsilon_{bypass} \leq 1$	0	-	
	Initial Temp.	T_{rfpl}	$T \geq T_{amb}$	°F	Case Dependent
UGS	Metal Mass	Mm2	0	lbm	3
	Water Mass	Mf2	0	lbm	3
	Flow Area	A2	0.9565	ft^2	3
	Height	L2	13.375	ft	
	Loss Factor	K2	2.173	ft	3, 5
Core	Metal Mass	Mm3	303800	lbm	
	Water Mass	Mf3	46488	lbm	
	Flow Area	A3	53.46	ft^2	
	Height	L3	12.917	ft	
	Loss Factor	K3	12.328	-	
	SDC flow rate	Q_{sdc}	0, 3000	gpm	Case dependent
	SDC inlet Temp	T_{sdcin}	75	°F	Case dependent
	Thermal Load	Q/Q_o	0.20	%	4, 8
Calculations	Time Step	Δt	< 15	Seconds	6
	Maximum Time	t_{max}	-	Minutes	
	Temp error	ΔT	< 0.5	°F	6
	Print	NPRT	> 0	print output	
	Print per time	$< N_{max}$	-		7
	Plot	NPLT	> 0	to .txt file	
	Plot per time	$<N_{max}$	-		7

See NOTES next page.

Notes for Table A-2
Input for CCNPP Units 1 & 2

Table A-2 Notes	
1	P_{amb} used in calculation of subcooled boiling temperature
2	$L_{eq} = A_{surface}$ / Wetted Perimeter
3	UGS removed; Loss factor & Area included for information only
4	$Q_o = 2754 \times 10^6$ watts-thermal = 9399×10^6 btu/hr
5	K= 6787 when based on core flow area of 53.46 ft^2
6	Number of time steps = $t_{max} * 60 / \Delta t = N_{max}$
7	Recommended values based on convergence study (0.10°F)
8	0.20% selected for test cases.

Table A-3
Sample Case Input Listing

Cases	SDC		SFP		RFP	Containment
	Q_{sdc}, gpm	T_{sdcln}, °F	Q_{sfp}, gpm	T_{sfpln}, °F	T_{sfpl}, °F	T_{amb}, °F
Case 1	3000	75	0	NA	75	75
Case 2	3000	75	1200	75	75	75
Case 3	0	NA	1200	75	75	75
Case 4	0	75	0	75	75	75

Q_{sdc} Shutdown Cooling System flow
T_{sdcln} Shutdown Cooling System inlet temperature
Q_{sfp} Spent Fuel Pool flow
T_{sfpln} Spent Fuel Pool inlet temperature
T_{sfpl} Initial Refueling Pool temperature
T_{amb} Containment ambient temperature

Table A-4
Output Parameters

PARAMETERS	VAR[A]	DEFINITION
As functions of Time		
Tcore (°F)	T_4	Core outlet Temperature
Tpool (°F)	T_6	Refueling Pool Temperature
Core (gpm)	$\dot{Q}$	Natural Circulation Flow Rate
Tpumpo (°F)	T_8	Spent Fuel Pool Outlet Temperature
Tavgc (°F)	$T_4 + T_8$	0.50 x (Tcore-in + Tcore-out)
Error Q(~)		
At the last time step		
Core Outlet Temperature (°F)	T_4	Core Outlet Temperature
Subcooled Boiling Temperature (°F)	T_{4SC}	Tsat = f (Pressure at top of core)
Pool Bulk Temperature (°F)	T_6	Refueling Pool Temperature
Surface Heat Loss[NC+Evap] (Btu)	Qsurf	Surface Heat Loss
Surface Natural Convection (Btu)	Qnc	Heat Loss due to Natural Convection
Evaporation (lbm)	Mevap	Amount of Surface Evaporation
Surface Evaporation (Btu)	Qevap	Heat Loss due to Evaporation
Spent Fuel Pool Pump Heat Load (Btu)	Qsfp	Total SFP Heat Removal
SDC Heat Load (Btu)	Q_1	Total SDC Heat Removal
Core Convection Heat Load (Btu)	Q_2	Convection Heat Transfer Core-RFP[1]
Qcoretotal = Qcstored + Qsdctot + Qcnctot (Btu)	Q_3	Total Heat Transfer from Core[1]
Qpooltotal = Qpstored + Qsfpumptot + Qnctotal(Btu)	Q_4	Total Heat Transfer from the RFP[1]
Decay Heat = Qd * Time (Btu)	Q_5	Total Heat Generation from Core[1]
Heat Balance: (Qcore - Qdecay) / Qdecay (%)	-	Change in Core Heat = Decay Heat
Heat Balance: (Qpool - Qnacore) / Qnccore (%)	-	Change in Heat to RFP = Core Convection
Time Constant (minutes)	τ_{rfp}	Time Constant for RFP Heat Up[2]

Note 1: Following heat balances must be satisfied: SDC + Core Convection: $Q_1 + Q_2 = Q_5$; Core convection = Decay Heat, $Q_2 = Q_4$.
Note 2: Time constant = $M_{RFP}/m_{natural\ circulation}$

[A] Variables in the analysis, see Table A-1.

Figure A-3
Sample Cases: Average Refueling Pool Temperature

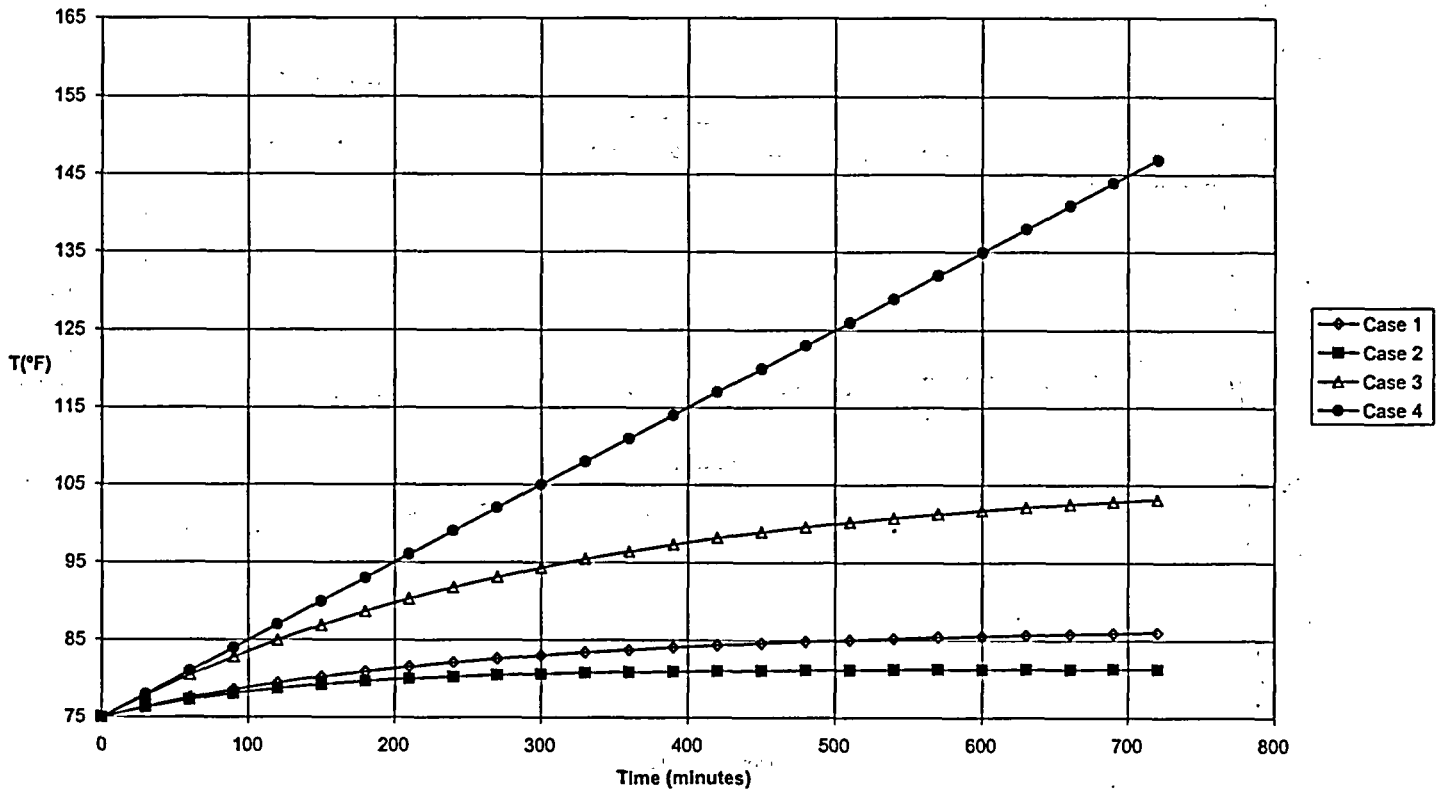

Figure A-4
Sample Cases: Natural Circulation Flow between Core and Refueling Pool

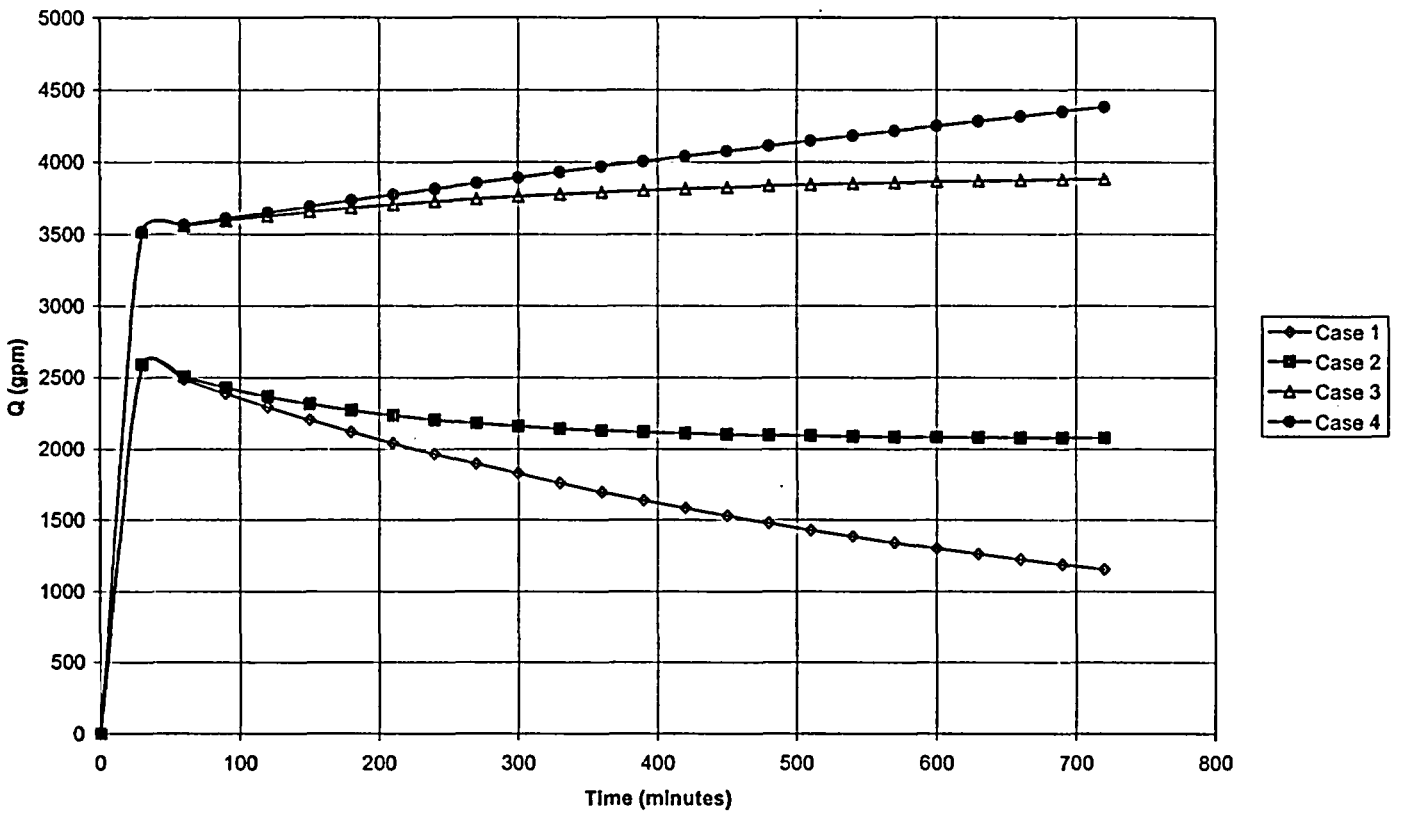

APPENDIX B

COMPARISON OF PREDICTIONS WITH TEST DATA

APPENDIX B
COMPARISON OF PREDICTIONS WITH TEST DATA

B.1 Test Data

Validation of the model developed in Appendix A is based on a comparison with data recorded at CCNPP Unit 2 during the March 2001 refueling outage. Under limited conditions, CCNPP units are permitted to use an alternate refueling pool cooling system during Mode 6 with the refueling pool flooded and with shutdown cooling secured. In this alternate cooling alignment a train of the spent fuel pool cooling system is manually aligned so that the spent fuel pool cooling pump takes suction from the refueling pool. After passing through the spent fuel pool cooling heat exchanger, the flow is directed back into the refueling pool. This flow is directed into the refueling pool through piping near the bottom of the pool (Figure B-1). The suction from the refueling pool to the spent fuel pool cooling line is through a drain in the bottom of the refueling pool, at the side of the pool opposite the inlet point.

Test data were recorded for two days during which the alternate pool cooling alignment was in use. Fluid temperatures in the refueling pool where recorded by thermocouples located at the reactor flange level, at mid-level in the pool, and close to the pool surface. Approximate locations of these thermocouples are noted in Figure B-2. Additional parameters recorded are listed in Table B-1.

The approximate time for initiation and securing of both shutdown cooling and refueling pool flows are listed in Table B-2. Measurements of flow rates and temperatures versus time, in days after shutdown (DAS) are shown in Figures B-3, B-4 and B-5.

Figure B-3 shows shutdown cooling flow rates, plus inlet (into the cold leg) and outlet (out of the hot leg) temperatures versus time. Note the reduction in shutdown cooling flow from 3000 gpm to 1500 gpm at about 6 days into the shutdown to facilitate flooding the refueling pool, and detensioning and removing the head. Once the head is removed, natural convection between the core and refueling pool starts. Thus predictions are only valid after the head is removed[1].

Figure B-4 gives ~~spent fuel pool~~ alternate heat removal cooling system flow rates and temperatures into the refueling pool and out of the refueling pool. These data were taken about 17 to 20 days into the outage. As shown in this figure, both the shutdown cooling system and the ~~spent fuel pool~~ alternate heat removal cooling system are activated near the start and end of the time period. This is to assure that the switchover into and out of the alternate alignment is successful.

Figure B-5 shows the average refueling pool temperatures at each of the three elevations. As expected, the fluid temperatures are highest at the reactor flange and decrease toward the pool surface.

[1] Heat removal via the SDC indicates a decrease of about 17% after removal of the head. This reduction is due to natural circulation flow between the core and refueling pool.

B.2 Comparison of Predictions with Test Data

Switching from the conventional shutdown cooling decay heat removal, both before and after the head is removed, followed by switching to the alternate decay heat removal are represented for the following cases:

Case 1: Reduce shutdown cooling flow for vessel head removal.
Case 2: Restore full shutdown cooling flow.
Case 3: Initiate alternate heat removal cooling flow, continue shutdown cooling flow.
Case 4: Secure shutdown cooling flow, continue alternate heat removal cooling flow.
Case 5: Secure alternate heat removal flow, restore shutdown cooling flow.

Temperatures and flow rates for these cases are listed in Tables B-3 and B-4. Predictions for shutdown cooling and spent fuel pool (alternate heat removal) outlet temperatures versus time, Figures B-6 and B-7, compare well with outage data. Time-averaged values of the shutdown cooling, spent fuel pool cooling (alternate heat removal) and refueling pool temperatures are compared in Table B-5. With the exception of Case 1, the predicted shutdown cooling and refueling pool temperatures are in reasonable agreement as shown in Figure B-8. The 10% difference in SDC predictions and data are related to uncertainties in decay heat values and initial refueling pool temperatures at the time the head is removed.

A comparison of predicted and measured average refueling pool temperatures is shown in Figure B-7. Experimental values are taken as the numerical average of the readings shown in Figure B-5. Agreement is good except for the initial portion where variations in the data are due to operator controlled changes in the SDC flow to reach an acceptable operating point.

Table B-1
Measured & Calculated Parameters based on CCNPP2 Data

MEASURED			CALCULATED
PARAMETER		DESCRIPTION	HEAT BALANCES
SFPin	T_{SFPI}	T-into the RFP	
SFPout	T_{SFPO}	T-out of the RFP	
SFPflow	M_{RFP}	Flow into the RFP	$Q_{RFP} = M_{RFP}C_P (T_{RFPO} - T_{RFPI})$
SWin	T_{SWI}	T-into SW-HX	
SWout	T_{SWO}	T-out of SW-HX	
SWflow	M_{SW}	Flow thru SW-HX	$Q_{SW} = M_{SW}C_P (T_{SWO} - T_{SWI})$
SDCout	T_{SDCI}	T-out of RV hot leg	
SDCin	T_{SDCO}	T-into RV cold leg	
SDCflow	M_{SDC}	Flow in SDC	$Q_{SDC} = M_{SDC}C_P (T_{SDCO} - T_{SDCI})$

Table B-2
Event Time Related to CNNP2 Outage

EVENT	DATE	TIME[a] (hr:min)	DAS (Days)	QDECAY (btu/hr)	DECAY HEAT[b] (%)	Refueling Pool Cooling Load
MODE 5	03/16/2001	23:55	0.000	2.264E+08	2.409%	Full Core
SDC start	03/19/2001	09:01	2.000	4.630E+07	0.493%	
HEAD removed	03/23/2001	04:30	5.750	3.089E+07	0.330%	
RFP start	04/03/2001	22:00	17.625	1.320E+07	0.140%	125 Assy
SDC secured	04/04/2001	13:00	18.208	1.303E+07	0.139%	
AHR steady-state	04/05/2001	00:00	18.715	1.290E+07	0.137%	
SDC restored[c]	04/07/2001	13:40	20.486	1.248E+07	0.133%	
AHR end data	04/07/2001	14:42	20.722	1.238E+07	0.132%	
RFP secured	04/08/2001	05:00	21.358	1.223E+07	0.130%	

a. Approximate times
b. Q_o = 9.399E+09 btu/hr
c. End of steady state period

Table B-3
Average Values Based on Experimental Data

CASE		TIME (hours)		TEMPERATURE (°F)					FLOW (gpm)		Qpower = 9.399E+09 (btu/hr)	
	Range	Tstart	Tend	SDC in	SDC out	SFP in	SFP out	RFP	Qsdc	Qsfp	Qdecay	%decay
1	Reduce SDC flow	0	11	73.58	102.90	NA	NA	NR	1521.87	0	2.034E+07	0.216%
2	Full SDC flow	11	285	92.01	102.73	NA	NA	NR	3071.05	0	1.572E+07	0.167%
3	SDC + AHR flow	285	298	99.00	103.30	92.03	96.78	101.30	3088.98	1195.65	1.313E+07	0.140%
4	AHR flow only	298	348	NA	NA	78.16	92.95	99.26	0	1194.23	1.276E+07	0.136%
5	SDC, AHR = 0	348	375	96.72	102.89	NA	NA	NR	0	0	1.231E+07	0.131%

NA = Not Applicable
NR = Not Recorded

Table B-4
Input for Algorithm Cases

CASE		TIME (minutes)		TEMPERATURE (°F)			FLOW (gpm)		Decay Heat
	Range	ΔTime	Time	SDC in	SFP in[3]	RFPi	Qsdc	Qsfp[3]	(%)
1	Reduce SDC flow	660	660	73.58	NA	75	1521.87	0	0.216%
2	Full SDC flow	16440	17100	92.01	NA	92.3[1]	3071.05	0	0.167%
3	SDC + AHR flow	780	17880	99.00	92.03	102.03[1]	3088.98	1195.65	0.140%
4	AHR flow only	3000	20880	NA	78.16	100.25[1]	0	1194.23	0.136%
5	SDC, AHR = 0	1680[2]	NA	NA	NA	99.52[1]	0	0	0.136%

1. RFP average temperature taken from prior Case.
2. Time when RFP temperature reaches 212°F.
3. SFP in, Qsfp refer to AHR flow.

Table B-5
Comparison between Predictions and CCNPP2 Data for Average Temperatures

	Tsdc-outlet (°F)		Tsfp-outlet (°F)		Trfp-average (°F)	
CASE	CALC	DATA	CALC	DATA	CALC	DATA
1	91.98	102.84	NA	NA	NA	NR
2	102.14	102.74	NA	NA	NA	NR
3	104.39	99.00	100.59	96.78	100.59	101.07
4	NA	No Data	99.60	92.95	99.60	99.23
Ref:	Figure A (next page)		Figure B		Figure C	

Figure B-4
CCNPP Unit 2 Outage Tests: Spent Fuel Pool Flow Rate and Temperature versus Time

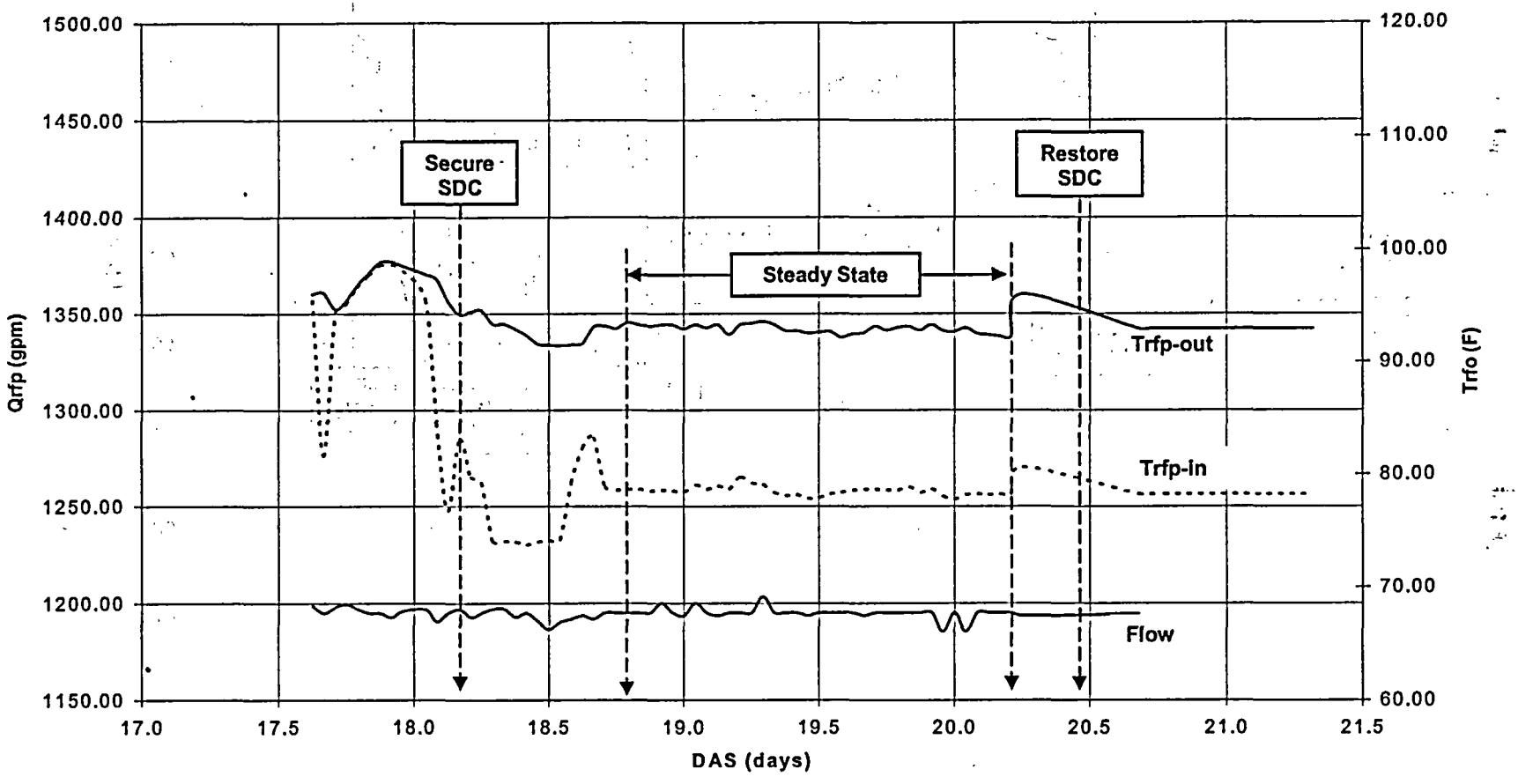

Figure B-5
CCNPP Unit 2 Outage Tests: Average Refueling Pool Temperatures versus Time

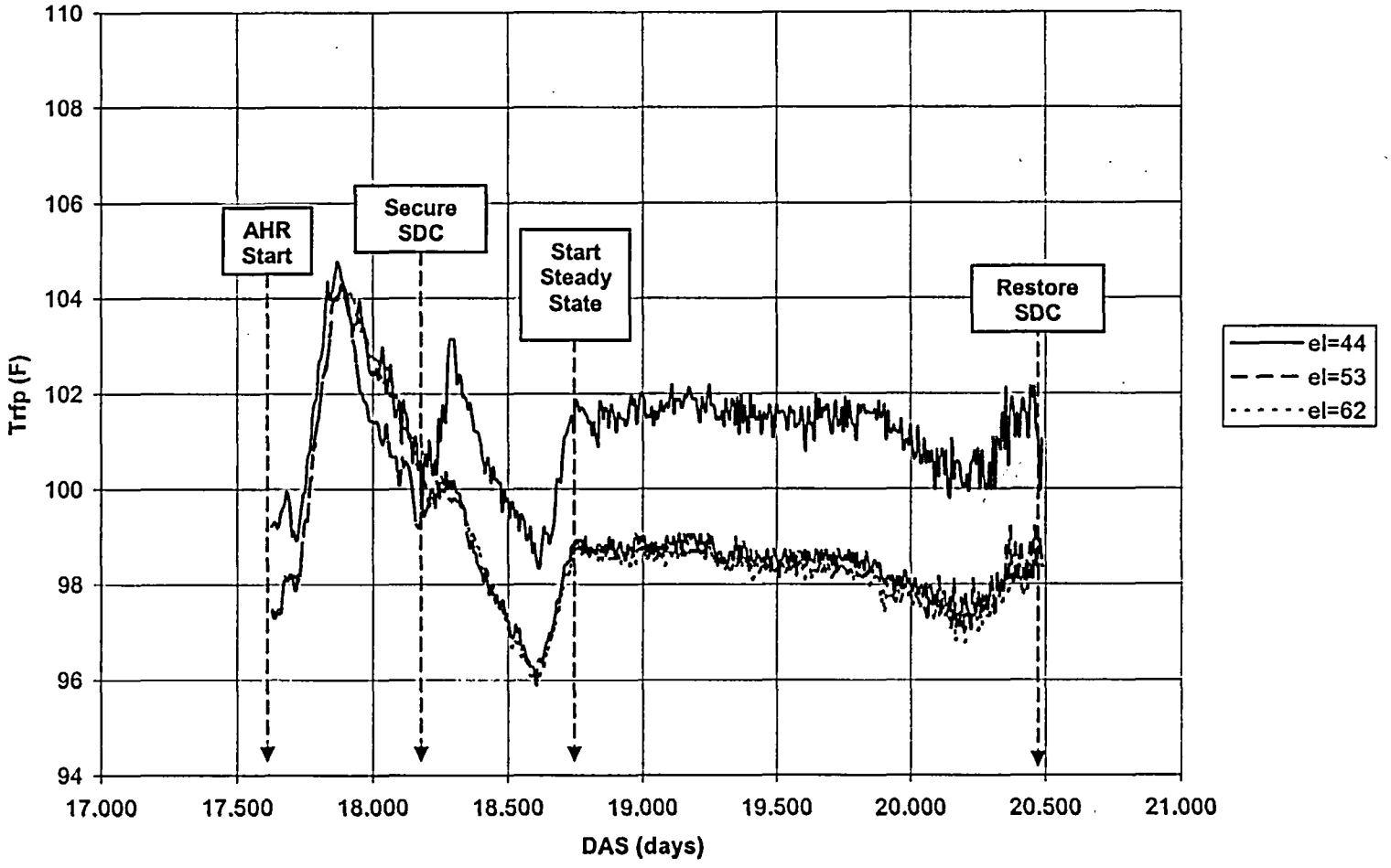

APPENDIX C

COMPARISON OF CCNPP UNIT 2 TEST DATA WITH COMPUTATIONAL FLUID DYNAMICS PREDICTIONS

APPENDIX C

COMPARISON OF DATA WITH COMPUTATIONAL FLUID DYNAMICS PREDICTIONS

This Appendix provides a comparison of CCNPP Unit 2 test data with predictions based on a computational fluid dynamic model of the refueling pool.

The geometry of the CFD model (Figure C-1) for the refueling water pool preserves the volumes of the refueling pool. Core flow rate and heat generation rate, from the lumped parameter model, are applied as boundary conditions.

Computational fluid dynamics computations based on a decay heat generation rate of 0.0946% predict a temperature difference between the refueling pool outlet and inlet of 15.0°F, approximately 1% above an average of the measured temperature difference of 14.82°F (Table C-1).

Refueling pool temperature data at different elevations above the reactor vessel flange indicates that the pool temperature decreases with elevation. This suggests that the hot plume from the core thermally mixes with the colder refueling pool water and cools as it rises to the top of the pool.

Computational fluid dynamics predictions of the refueling pool water temperatures at locations corresponding to the measurement points compare favorably with the measured temperatures, as shown in Table C-1. In general, computational fluid dynamics predictions are higher than measured values. The highest differences occur in the SE-NE quadrants (0° to 180°) due to a non-uniform distribution of the inlet (in the 180° to 270° quadrants) to outlet (in the 270° to 360° quadrants) over the reactor. (Refer to Figure B-2 for quadrant orientation.) Measurements being lower than predictions indicate a higher degree of mixing and a more uniform distribution of inlet flow than predicted by the computational fluid dynamics model.

Features of thermal hydraulic mixing in the refueling water pool are depicted in Figures C-2 and C-3, which show the temperature distribution of the thermal plume from the core in a vertical plane and through a series of horizontal planes. (Note: the temperature scale shown is in degrees Rankine; subtract 460 to obtain Fahrenheit). These temperature distributions illustrate the thermal plume rising above the core and then being transported downstream toward the drain. In Figure C-3, the bias of flow around the core to the SW and NW result in the lower temperatures predicted for those two locations.

Predicted values of fluid temperatures decrease with rising elevation above the vessel and are higher on the downstream side (angles of 45° and 135°) than the upstream side (angles of 225° and 315°). These differences are due to ~~spent fuel pool~~ heating of the alternate cooling flow as it crosses the core and mixing not being as complete in the CFD model as in the refueling pool. Predicted values are, on the average, about 3% higher than measurements.

In general, the thermal plume is predicted to rapidly mix in the vertical direction while the cavity of the pool that is associated with the incoming core flow remains cold. Some of this cold mass does short-circuit the core to the cavity on the drain side. Within the drain

cavity, the pool temperature is warmer and reduces to the drain temperature at 94°F. At the surface of the pool, the maximum temperature is 103°F and the volume weighted average temperature is 94°F. As noted from Figure C-4, the test data shows temperatures are more uniform in the vertical direction than those predicted by the computational fluid dynamics model.

Circulation due to the thermal plume results in the predicted values for fluid velocity in the vertical plane (Figure C-5) and horizontal plane (Figure C-6) being the highest in the region above the reactor flange. These velocity profiles above the core are an indication of the strong mixing and recirculation occurring in that region. CFD results show the highest fluid velocity in the natural circulation plume to be approximately 0.2 feet/second.

~~The highest fluid velocities, of about 0.2 ft/second, occur in the region above the core. Since the thermal plume is turbulent, there is also an additional fluctuating velocity component of approximately 0.02 ft/second. The mean and the fluctuating velocities result in a maximum velocity of 0.22 ft/second. The largest vertical velocities, of about 0.2 ft/second, occur near the refueling pool drain.~~

Table C-1
Comparison of Thermocouple Data with Computational Fluid Dynamics Predictions

Location	TEMPERATURES (°F)													
Direction	NE		SE		SW		NW		Average		Alternate Cooling Flow			
Angle	45°		135°		225°		315°				IN		OUT	
Elevation	DATA	CFD	DATA	CFD	DATA	CFD	DATA	CFD	DATA	CFD	DATA	CFD	DATA	CFD
44-ft	101.42	108.71	101.31	107.68	101.93	100.78	100.74	102.95	101.35	105.03	78.82	78.57	93.39	93.57
53-ft	99.49	101.34	98.30	101.70	97.50	93.73	98.71	95.05	98.50	97.96				
62-ft	98.77	100.69	98.57	101.75	97.72	97.55	98.77	98.51	98.46	99.63				

Refer to Figure B-2 for quadrant orientation.

APPENDIX D

EVALUATION OF ALTERNATIVE HEAT REMOVAL ALIGNMENTS

APPENDIX D
EVALUATION OF ALTERNATIVE HEAT REMOVAL ALIGNMENTS

The objective of this Appendix is to document predictions of fluid temperature at a value of 0.315% decay heat, seven days after reactor shutdown, considering four alternatives for location of the inlet and suction. In all cases the analysis is based on the parameters for the CCNPP refueling pool /reactor cavity geometry.

D.1 REACTOR CAVITY CONFIGURATIONS

The four configurations to be analyzed are described in Table D-1, shown schematically in Figure D-1. The selection of configurations were chosen to represent a variety of possible conditions that may exist and that none of these configurations represent the exact configuration of the CCNPP units when they are aligned for alternate heat removal. The analyzed configurations are identified as follows:

Configuration A: Alternate Piping: Suction across core.
Configuration B: Alternate Piping: Suction same side.
Configuration C: Transfer Tube: Suction across core.
Configuration D: Transfer Tube: Suction on same side.

The influence of the different flow paths on the one-dimensional model is manifested through the mixing and bypass coefficients. To evaluate these coefficients, computational fluid dynamics models are prepared for each of the configurations. The following are the assumptions used for these one-dimensional evaluations:

- Containment temperature = 100°F
- Inlet temperature = 85°F
- Decay heat = 0.315% (seven days after shutdown)
- ~~Spent fuel pool~~Alternate heat removal flows; 200 gpm and 2000 gpm

D.2 ONE-DIMENSIONAL MODELING

The one-dimensional computational fluid dynamics model uses mixing and bypass coefficients to incorporate the mixing of the core flow with the reactor cavity fluid and the alternate cooling flows. The mixing coefficient, ε_{mix}, accounts for the portion of the reactor cavity fluid that does not mix (remains close to the initial pool temperature) with the core flow. The bypass coefficient, ε_{bypass}, accounts for the~~spent fuel pool~~ alternate heat removal flow that does not mix (remains close to the inlet temperature) with the core exit flow. The bypass flow path is shown schematically for Configuration A in Figure D-2.

The one-dimensional model assumes values for the mixing and bypass coefficients. This model is independent of locations of the inlet and drain for the alternate cooling paths. Thus, computational fluid dynamics models of the various arrangements must be used to re-evaluate these coefficients for use, in what is an iterative procedure, in the next one-dimensional model calculations.

The relationship between the definition of the mixing coefficient and temperatures in the computational fluid dynamics model is~~derived outside this text~~ shown below. The mixing

coefficient is expressed in terms of the pool average temperatures for the one-dimensional and computational fluid dynamics analyses as,

$$\varepsilon_{mix} = M / M_6 = (\overline{T}_{CFD} - T_i)/(\overline{T} - T_i)$$

where T_i is the initial pool temperature.

The bypass coefficient represents the fraction of the ~~spent fuel pool~~ alternate heat removal cooling flow that does not mix with the flow out of the core. Conservation of energy for the mixed and unmixed flows then gives the outlet temperature for this flow as,

$$(1-\varepsilon_{bypass})m_{sfp}c_p\overline{T} + \varepsilon_{bypass}m_{sfp}c_pT_{pi} = m_{sfp}c_pT_{po}$$

The bypass coefficient is solved for as,

$$\varepsilon_{bypass} = (\overline{T} - T_{po})/(\overline{T} - T_{pi})$$

where $\overline{T}$ is the pool average temperature for either the one-dimensional or computational fluid dynamics models. For the computation fluid dynamics model, the alternate heat removal cooling flow that does not mix with the core plume flow is,

$$\varepsilon_{bypass,CFD} = (\overline{T}_{CFD} - T_{po,CFD})/(\overline{T}_{CFD} - T_{pi})$$

where po and pi refer to the refueling pool outlet (drain) and inlet temperatures.

~~The one-dimensional evaluations based on perfect mixing, that is, those with a mixing coefficient of 1.0 and a bypass coefficient of 0.0, are summarized in Table D-2. All results use the assumed value of 0.315% for the decay heat. Case 4 and Case 5 use flow rates of 2000 and 200 gpm for the spent fuel pool flow. The core flow rates of 8563 gpm and 10408 gpm, respectively, for these cases are boundary conditions for the computational fluid dynamics evaluation.~~

~~Results for the one-dimensional evaluation with spent fuel pool flow of 2000 gpm for the influence of mixing and bypass coefficients is show in Table D-3. The variation with mixing coefficient, Cases 1-4, is negligible, whereas, the variation with bypass coefficients, Cases 5-7 is significant. Case 8 varies both the mixing coefficient (0.50) and the bypass coefficient (0.50) resulting in pool temperatures close to 150°F; the results for Cases 6 and 8, each with 0.50 mixing coefficient, are the same.~~

A one dimensional calculation with the mixing coefficient equal to one and the bypass coefficient equal to zero is used to determine the core flow rate that is applied as a boundary condition to the computational fluid dynamic evaluation of the alternate cooling flow alignments. For an assumed 0.315% decay heat level, the predicted core flow rates for alternative cooling flow rates of 200 and 2000 gpm are 10408 and 8563 gpm, respectively.

D.3 COMPUTATIONAL FLUID DYNAMICS MODEL EVALUATION

The mixing coefficient is meant to represent the influence of a non-uniform distribution of fluid temperature on the transient behavior of the fluid in the reactor cavity. The bypass coefficient is intended to represent the alternate cooling flow that may not transport heat from the core. It is assumed that the mixing and bypass coefficients are independent. Thus, the mixing coefficient may be determined based on no transport flow into or out of the cavity. However, evaluation of the bypass coefficient is dependent on the flow rate and the pool configuration. Results of this evaluation, based on the following core flow rates corresponding to the one-dimensional flow rates for perfect mixing, $\varepsilon_{mix} = 1$, and no bypass, $\varepsilon_{bypass} = 0$, cases are shown in Tables D-2 and D-3.

AHR flow rate ~~SFP~~ = 200 gpm Qcore = 10408 gpm
AHR flow rate ~~SFP~~ = 2000 gpm Qcore = 8563 gpm

Inlet flow to the refueling water pool from the ~~spent fuel pool~~ alternate heat removal flow path ~~cooling system~~ may be introduced from either a pipe at the upper surface of the pool or from a low-level inlet ~~the transfer duct low~~ in one of the pool cavities. Cooling flow may exit the pool through one drain which may be in either pool cavity. Since the CCNPP pool is nearly symmetric, four configurations bound the general possibilities for inlet and exit flow locations. For each inlet location, the drain location may be in the same cavity or in the cavity on the opposite side of the reactor vessel. With the inlet and exit in the same cavity, the ~~spent fuel pool~~ alternate heat removal cooling flow may short circuit the reactor vessel. With the inlet and exit on opposite sides of the reactor vessel, the ~~spent fuel pool~~ alternate heat removal cooling flow must at least pass by the open vessel. The slight non-symmetry of the refueling water pool, principally due to different depths of the cavities and the off-center location of inlets, should not be significant to these computations. These configurations are defined in Table D-1 and shown schematically in Figure D-1.

Results of this analysis, in the form of temperature profiles for the four configurations at the 2000 gpm alternate heat removal ~~spent fuel pool~~ flow rate, are shown in Figures D-3 to D-6.

D.4 BYPASS AND MIXING COEFFICIENTS

Results for the bypass coefficients are documented in Table D-2. For Configuration A, the flow that crosses the core and mixes with the flow from the core is reflected in a value of the bypass coefficient of about zero for both high and low ~~flow spent fuel pool~~ alternate heat removal flow rates. In contrast, for Configuration B the majority of the alternate heat removal flow goes directly to the drain, which is reflected in values of the bypass coefficients ~~less~~ close to unity.

Configurations C and D represents the arrangement where the alternative cooling path enters the refueling pool from a low level, such as through the fuel transfer tube. In Configuration C the flow is forced up and over the core. Computational fluid dynamics analysis ~~results~~ indicates that forcing the flow across the core results in the inlet flow into the core being closer to the spent fuel pool ~~cooling system flow~~ temperature of 85°F rather than the refueling pool average temperature assumed in the one-dimensional analysis. For this case, the resulting temperature of the flow out of the core is predicted to be lower than the average pool temperature. ~~and results in a value of the bypass~~

~~coefficient greater than one. The same is observed, though to a lesser extent, at the lower spent fuel pool flow, where the bypass coefficient is closer to one.~~

In the alternate cooling mode, decay heat is transported by natural circulation from the core into the refueling pool. A bypass coefficient having a value greater than zero denotes that a portion of the alternate cooling flow bypasses the natural circulation thermal plume above the core. For example, the alternate heat removal cooling inflow in Configuration B enters near the pool surface with the drain at the bottom of the refueling pool on the same side as the inlet. The temperature distribution for this configuration, shown in Figure D-4, suggests that most of the alternate cooling inflow only mixes with refueling pool water on the inlet side of the pool then exits the pool without significant mixing with the core thermal plume. Thus, a bypass coefficient greater than zero represents a reduction in the alternative cooling flow that interacts to remove decay heat from the core thermal plume and results in a higher pool average temperature, Tcfd, as shown in Table D-2.

~~The bypass coefficient represents the flow that is not effectively used to remove the decay heat, transported by natural circulation from the core, from the reactor cavity. Values less than one zero denote that a portion of the inflow from the alternate cooling path, in this case the spent fuel pool cooling system, is not used to remove this heat. For example, in Configuration A, the spent fuel pool alternate heat removal cooling inflow enters at the free surface with the drain at the bottom on the opposite side of the core. Here the temperature distribution, as shown in Figure D-3, shows that a portion of the inflow forms a recirculation at the bottom of the reactor cavity on the same side as the inflow. This, and a portion of the flow that may not mix with the natural circulation from the core, reduces the flow that can effectively remove the decay heat, resulting in higher outlet temperatures at the refueling pool drain.~~

In Configuration C the flow enters through a low-level location such as the transfer tube and exits through a drain at the bottom on the opposite side of the core. The temperature distribution in Figure D-5 shows a portion of the flow entering from the low-level inlet ~~transfer tube~~ remains near the bottom of the cavity; but most of the flow goes up and over the core. This cooler flow mixes directly with the natural circulation from the core before being drawn to the outlet. The higher rate of cooler flow passing by the core inlet results in lower values of core outlet temperatures. This may be reflected in the one-dimensional model by a value of the bypass coefficient less than zero, which is equivalent to increasing the mass flow entrainment of ~~spent fuel pool~~ alternate heat removal flow in the one-dimensional model.

Results for Configuration D, where the drain is on the same side as the ~~transfer tube~~ low level inlet, are similar to Configuration B. In both cases, the ~~spent fuel pool~~ alternate heat removal cooling flow short-circuits directly to the reactor cavity drain. The thermal effects of this short-circuiting are manifested in low temperatures in the path between the ~~spent fuel pool cooling system~~ alternate heat removal inlet and outlet and relatively higher temperatures elsewhere (Figures D-4 and D-6). Configurations B and D remove heat from the vicinity of the reactor core through the action of recirculation currents and turbulent diffusion in the active cavity of the refueling water pool that are produced by the natural circulation plume resulting from the core heat generation.

Values of the mixing coefficients are all close to unity. Based on this data, a value of 0.90, close to the minimum value of 0.88, was selected ~~is recommended~~ for use with the one-dimensional model.

Table D-1
Refueling Water Pool Cooling Configurations

Configuration	Inlet Location	Drain Location
A	Pipe flow directed downward in upper corner of pool	Drain in floor of cavity on opposite side of reactor vessel
B	Pipe flow directed downward in upper corner of pool (same as A).	Drain in floor of cavity on same side of reactor vessel
C	Transfer tube ~~duct~~ (low elevation in the pool)	Drain in floor of cavity on opposite side of reactor vessel
D	Transfer tube ~~duct~~ (low elevation in the pool)	Drain in floor of cavity on same side of reactor vessel

Refer to Figure D-1 for a schematic of these configurations.
Note that these configurations do not represent the specific configuration of the pool at the CCNPP Units.

Table D-2
CCNPP Unit 2 Bypass Coefficients Based on CFD Analysis

Config	A		B		C		D	
Flow(gpm)	2000	200	2000	200	2000	200	2000	200
Ti (°F)	85	85	85	85	85	85	85	85
Tsfp (°F)	85	85	85	85	85	85	85	85
Tmax (°F)	138.3	396.8*	170.1	444.6*	134.4	397.9*	193.8	421.8*
Tcfd (°F)	114.3	371.4*	149	418.9*	104.9	369.6*	156	393*
To (°F)	115	383.8*	110.3	377.3*	115	383*	108.9	382.7*
Tsurf (°F)	115.5	376.3*	149.3	423.9*	110.7	376.7*	166	400.8*
θ_{bypass}	-0.024	-0.043	0.605	0.125	-0.508	-0.047	0.663	0.033

* i.e., 200 GPM is insufficient to prevent boiling for the decay heat used.

Table D-3
CCNPP Unit 2 Mixing Coefficient Based on CFD Analysis

Analysis	Computational Fluid Dynamics			1-D
Location	Core Exit	Pool Surface	Pool Bottom	Uniform
Time (min)	750	833	874	886
Tsaturation (°F)	215	214	212	214
Taverage (°F)	197	209.4	215.5	212
ε_{mix}	0.88	0.98	1.03	1.0

Figure D-2
Flow Paths for Bypass Flow

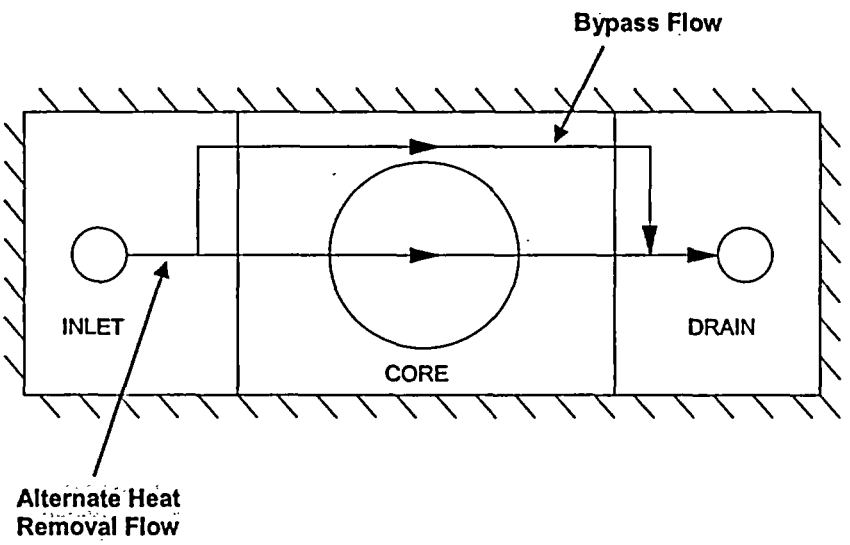

APPENDIX E

CCNPP SPECIFIC EVALUATION OF CONDITIONS FOR ALTERNATE DECAY HEAT REMOVAL IN MODE 6

APPENDIX E

CCNPP SPECIFIC PARAMETRIC EVALUATION OF CONDITIONS FOR ALTERNATE DECAY HEAT REMOVAL IN MODE 6

This appendix presents the results of several evaluations testing the sensitivity of various parameters on performance of normal decay heat removal and the alternate heat removal alignment for the CCNPP Units. Limits on the use of the alternate alignment for the removal of decay heat, while removing one or both trains of shutdown cooling from service, and the possibility of moving fuel, all depend on the temperatures in the refueling pool. At CCNPP Units 1 and 2 the alternate heat removal alignment is accomplished with a train of the spent fuel pool cooling system (FPCS). Hard piped connections from the FPCS are available to establish dedicated coolant circulation with the refueling pool.

Per Section 4.0 of the body of this report, the limits on the use of the alternate alignment for the removal of decay heat, while removing one or both trains of shutdown cooling from service, and moving fuel, depend on the temperatures in the refueling pool. The refueling pool temperature, in turn, depends on the ability of the aligned cooling systems to reject heat to the ultimate heat sink. This heat rejection is a function of the performance of the heat exchangers used to reject the heat and the heat sink temperature (T_{HS}). Limits on refueling pool temperatures are discussed in Section 4.1. Steps in determining refueling pool temperatures for values of heat sink temperatures are outlined in Section 4.2.

Removal of one or both trains of shutdown cooling from service will be limited by the fluid temperature reaching some value that represents the margin between the selected value and the core becoming uncovered. For the CCNPP Units the operating limit has been set at a value of 140°F, coincident with the limiting temperature for the spent fuel pool.

Temperatures and time to reach specific temperature limits can be predicted based on the one-dimensional, lumped parameter algorithm developed to predict refueling pool and core outlet temperatures versus time as described in Section 2.2. The algorithm contains provisions for the usual Mode 6 shutdown cooling alignment as well as an alternate alignment utilizing spent fuel pool cooling.

Fuel assembly movement during refueling operations can depend on local fluid velocities due to the thermal convection between the core and refueling pool and subsequent mixing with the local pool fluid circulation. The limiting fluid velocity is such that it is below values at which the fuel assembly can become tilted and difficult to insert into the core.

Changes in the Technical Specifications, discussed in Section 5.0, needed to support implementation of alternative heat removal and evaluation of limiting conditions for operation to meet these requirements, include:

- Conditions under which the alternate heat removal alignment may be used.

  Limiting conditions are a function of decay heat as a function of days after shutdown, refueling pool temperature as a function of heat sink temperature, flow rate and inlet temperature for the alternate heat removal alignment (Section E.1).

- Requirements for removing the shutdown cooling system from service.
- Time limits for interrupting the alternate heat removal flow.

  Limiting conditions for operation are based on time to reach a limiting value of refueling pool temperature (Section E.4).

- Fuel movements allowed when using alternate heat removal alignment.

  Limiting conditions for operation are based on fluid velocities induced by natural convection, in the region above the core, and the influence of the resulting fluid forces on alignment of the fuel assembly with its core location (Section E.5).

The following outlines the procedures and methodology for determining the above conditions. Values presented are based on calculations for CCNPP Unit 2.

E.1. RFP Temperatures vs. Inlet Temperature

With the head off, at assumed times after shutdown, the refueling pool (RFP) temperature is a function of the decay heat, shutdown cooling (alternate heat removal) flow and inlet temperature, and refueling pool initial temperature.

$$T_{RFP} = f(Q_{decay}, m_{SDC}, T_{SDCI}, T_{RFPi})$$

Decay Heat: Based on assumed values of time after shutdown, values of decay heat are obtained from the decay heat curve, assumed for conservatism, for a full core, for example Figure E-1.

Conventional Decay Heat Removal: Values are calculated for refueling pool temperature versus time, at different values of days after shutdown, and constant values of shutdown cooling system flow (3000 gpm), inlet temperature (90°F) and initial refueling pool temperature (90°F), for example in Figure E-2. The values of steady state temperatures, in this case at a constant value of T_{SDCI} of 90°F, are shown in Figure E-3.

~~The calculations are repeated for values of T_{SDCI} representing the expected high and low limits.~~

E.2. RFP Temperatures vs. Heat Sink Temperature

Alternate Decay Heat Removal: Values of the spent fuel pool temperature, TSFPi, are a function of the performance characteristics of the heat exchanger(s) used to remove

heat from the refueling pool and the final (ultimate) heat sink. Thus, upon switching to the alternate cooling alignment, at assumed times after shutdown, the refueling pool temperatures are calculated as a function of the decay heat, spent fuel pool (alternate heat removal) cooling system flow rate and inlet temperature and steady state temperature of the refueling pool at the time of the switch-over:

$$T_{RFP} = f(Q_{decay}, m_{SFP}, T_{HS}, T_{RFPI})$$

Predicted values of refueling pool temperatures versus time, are shown in Figure E-4 and steady state values in Figure E-5. Both figures are based on a heat exchanger effectiveness and flow, multiplied by specific heat ratio, Cr, of one, so that TSDCi = THS.

As with conventional heat removal the calculation is repeated for values representing the expected high and lower limits of the heat sink temperature, THS.

Limiting THS vs. TAS: Repeated calculations for RFP temperatures result in a family of curves such as shown in Figure E-4. Refueling pool equilibrium temperatures will decrease with lower values of heat sink temperature and increase with higher values of heat sink temperatures. Selection of a limiting value of refueling pool temperature results in the time after shutdown that the alternate heat removal alignment can be aligned and not exceeds this limit. For a limiting value of 140°F, based on Figure E-5, the limiting condition of operation for entering alternate heat removal alignment with a 90°F heat sink temperature is about 5 days.

E.3. Time to Reach Limiting Temperatures

Results in Figure E-5 show that, for CCNPP Unit 2, the alternate heat removal alignment is sufficient to keep the refueling pool temperatures below the values of both the selected limiting value of 140°F and saturation (212°F) temperatures. However, the time to reach saturation decreases the higher the steady state values of the refueling pool temperatures. With loss of alternate heat removal alignment, refueling pool temperature versus time, for a constant value of heat sink temperatures, is a function of the decay heat and temperature of the pool at the time alternate heat removal cooling is lost;

$$T_{RFP} = f(Q_{decay}, T_{RFPI})$$

Refueling pool temperature as a function of time, at constant values of days after shutdown is shown in Figure E-6. Parametric relationships between the time, Δt, to reach, either the limit on SFP temperature of 140°F or a value of 212°F, are shown in Figure E-7.

$$\Delta t = f(DAS, Q_{decay}, m_{SFP}, m_{SDC}, T_{SFPI}, T_{SDCI}, T_{RFPI})$$

The outage schedule calls for initiation of alternate heat removal alignment from 15 - 25 days into the shutdown, for a duration of 5 days. Times to reach limits on temperature during this operating period are as follows:

Footnote 1 has been deleted.

Time into Shutdown (Days)	Time to Reach Temperature Limits (hours)	
	140°F	212°F
15	1.67	13.3
25	6	16.7

E.4. Fuel Movement

Fuel movement depends on fluid velocities due to the thermal convection between the core and refueling pool and subsequent mixing with the pool circulation flow. The fuel assembly can become tilted and difficult to insert into the core when these local fluid velocity values are below limits. The limiting condition can be determined as follows.

Tilt Angle: With reference to Figure E-8, the horizontal component of drag force on a fuel assembly titled from vertical by an angle θ is given by:

$$F_D = \frac{C_D}{2}\rho V^2 \cdot A_P \cos\theta$$

where C_D is the drag coefficient, ρ the fluid density in units (lbm/ft^3), V the average velocity over the length of the bundle, in units (ft/sec), A_P the projected surface area (bundle height times width) of the bundle, in units (ft^2).

Upon equating the drag force, the component of weight in the same direction as the drag component,

$$\frac{C_D}{2}\rho V^2 \cdot A_P \cos\theta = M_{FA} g \cdot \sin\theta$$

where M_{FA} is the mass, in units (lbm), of the fuel assembly and g the acceleration of gravity (32ft/sec^2). The tilt angle is then given by,

$$\theta = \tan^{-1}\left[\frac{C_D \rho V^2 A_P}{2 M_{FA} g}\right]$$

This relationship is shown in Figure E-9.

Evaluation: The maximum value of 2.4 for the drag coefficient, is based on the assumption of the fuel assembly being modeled as an infinite beam, with a square cross section rotated 45° to the flow. The density, based on a refueling pool temperature of 100°F, is 62.4 lbm/ft^3. Tilt angle as a function of fluid velocity is shown in Figure E-10. While the angles are small, the limiting value will depend on plant specific experience with insertion of fuel assemblies during refueling.

Fluid Velocity: Based on the CFD analysis ~~in Reference 6.4~~, the maximum velocity occurs in the thermal plume region above the core. Furthermore, the velocities tend to

be higher the closer to the top of the vessel. Based on the assumption that the velocities are proportional to the natural convection flow, Q_{NC}, from the vessel, the velocity is,

$$V_{max} = Q_{NC}/A_{FLOW}$$

Based on the model in Figure E-11, the flow area corresponds to a circular flow area of about 6 feet in diameter, which corresponds to about half the flow area at the top of the vessel.

Predictions based on the one-dimensional model, of flow rate due to natural convection between the core and refueling pool, of 2900 gpm result in a velocity of about 0.2 feet per second. Review of the CFD analysis indicated that the velocities in both the vertical and radial directions are about equal.

Limiting Conditions: Values of tilt angle as a function of time after shut down is calculated as follows.

The natural convection flow rates between the core and the refueling pool is a function of the decay heat, Figure E-1. Corresponding flow rates as a function of days-after-shutdown, DAS, are shown in Figure E-12.

Based on these flow rates, maximum velocity as a function of DAS is calculated from,

$$V_{max} = Q_{NC}/A_{FLOW}$$

where A_{FLOW} is taken as 29 ft^2.

Corresponding values of tilt angle can then be computed based on the following relationship.

$$\theta = \tan^{-1}\left[\frac{C_D \rho V^2 A_P}{2 M_{FA} g}\right]$$

Limiting values of tilt angle will depend on plant specific experience with fuel assembly insertion. Values of velocities and corresponding tilt angles are shown in Figure E-13.

The allowable window for initiation of AHR should be based on temperature limits and then determine if the tilt angles are sufficiently small so as not to result in problems with insertion of fuel assemblies.

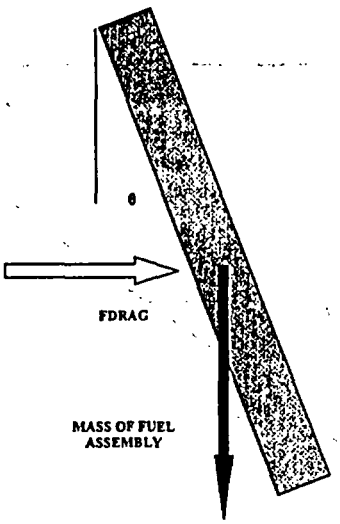

Figure E-8
Limiting Conditions for Moving Fuel

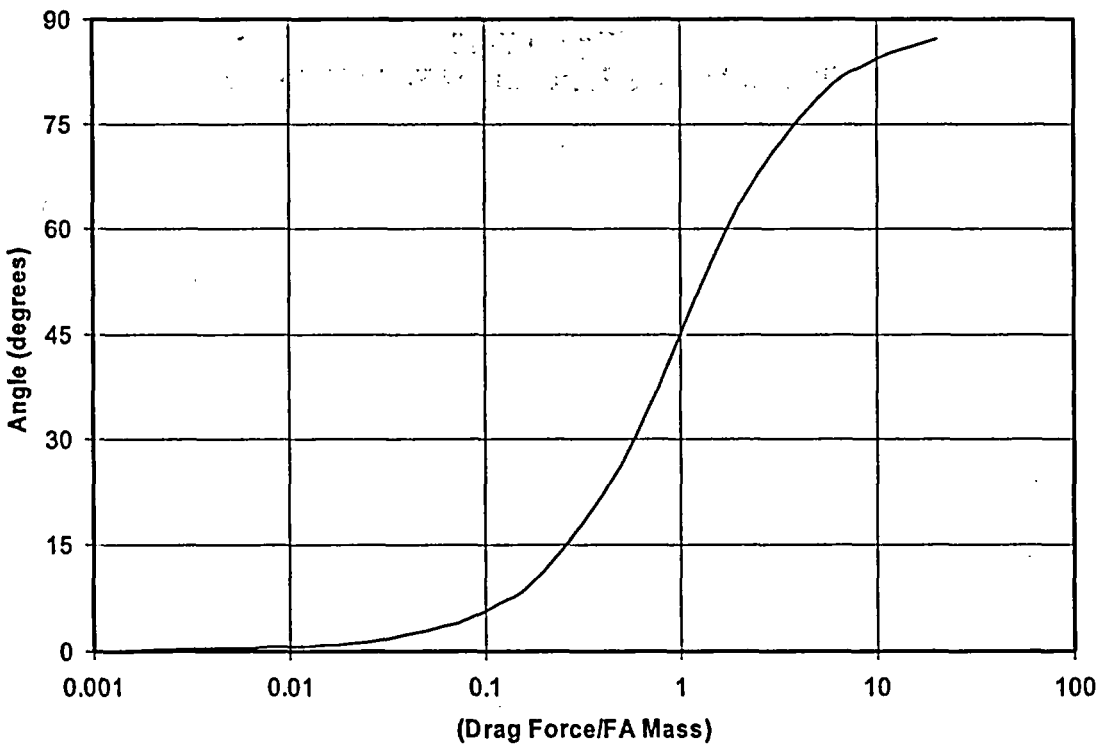

Figure E-9
Tilt Angle as a Function of the Ratio of Drag Force to Fuel Assembly Mass

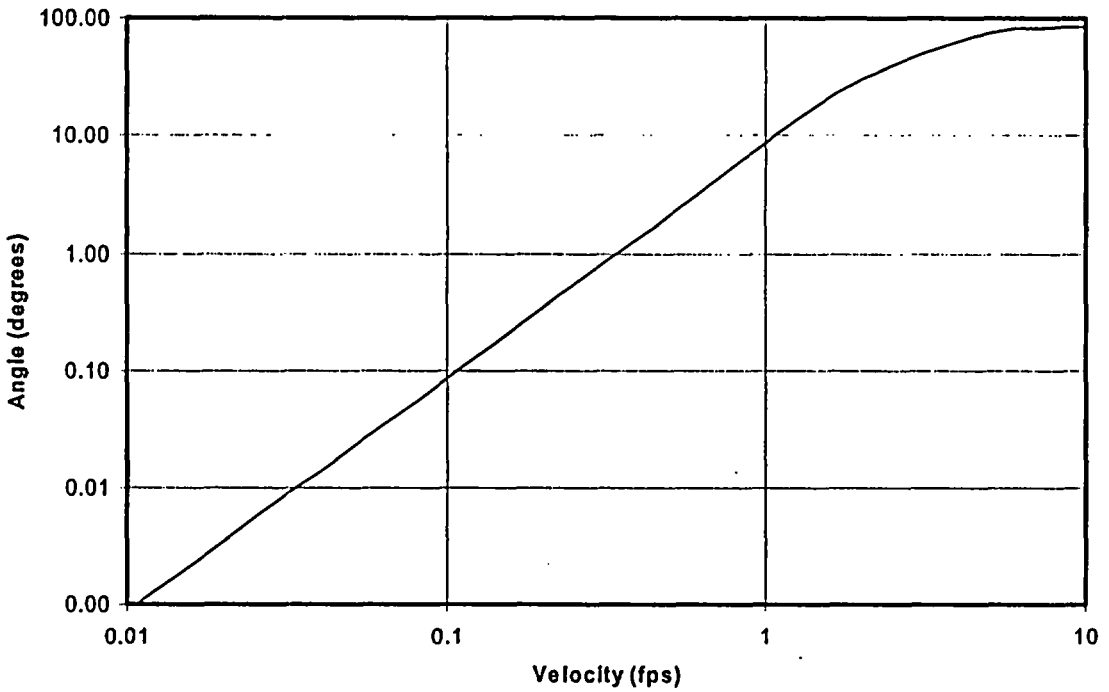

Figure E-10
Tilt Angle as a Function of Fluid Velocity

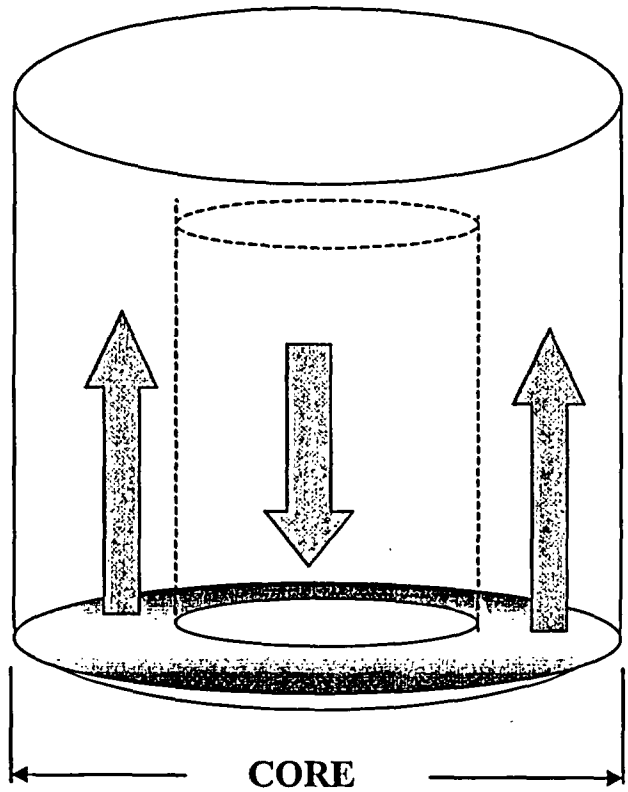

Figure E-11
Flow Areas for Natural Convection Flow

WCAP-15872-NP

End of Change Pages